



HAL
open science

Earth's Rotation: Observations and Relation to Deep Interior

Jérémy Rekier, Benjamin F Chao, Jianli Chen, Véronique Dehant, Séverine Rosat, Ping Zhu

► **To cite this version:**

Jérémy Rekier, Benjamin F Chao, Jianli Chen, Véronique Dehant, Séverine Rosat, et al.. Earth's Rotation: Observations and Relation to Deep Interior. Surveys in Geophysics, In press, 10.1007/s10712-021-09669-x . hal-03451262

HAL Id: hal-03451262

<https://hal.science/hal-03451262v1>

Submitted on 26 Nov 2021

HAL is a multi-disciplinary open access archive for the deposit and dissemination of scientific research documents, whether they are published or not. The documents may come from teaching and research institutions in France or abroad, or from public or private research centers.

L'archive ouverte pluridisciplinaire **HAL**, est destinée au dépôt et à la diffusion de documents scientifiques de niveau recherche, publiés ou non, émanant des établissements d'enseignement et de recherche français ou étrangers, des laboratoires publics ou privés.

See discussions, stats, and author profiles for this publication at: <https://www.researchgate.net/publication/356219741>

Earth's Rotation: Observations and Relation to Deep Interior

Article in *Surveys in Geophysics* · November 2021

DOI: 10.1007/s10712-021-09669-x

CITATIONS

0

READS

77

6 authors, including:



Jérémy Requier

Royal Observatory of Belgium

20 PUBLICATIONS 109 CITATIONS

[SEE PROFILE](#)



Veronique Dehant

Royal Observatory of Belgium

534 PUBLICATIONS 6,550 CITATIONS

[SEE PROFILE](#)



Severine Rosat

University of Strasbourg

114 PUBLICATIONS 1,493 CITATIONS

[SEE PROFILE](#)

Some of the authors of this publication are also working on these related projects:




SovaP on Picard [View project](#)



Geo- and space instrumentation design [View project](#)



1 Earth's Rotation: Observations and Relation to Deep Interior

2 **Jérémy Rekier**¹  · Benjamin F. Chao¹ · Jianli Chen¹ · Véronique Dehant¹ ·
3 Séverine Rosat¹ · Ping Zhu¹

4 Received: 19 May 2021 / Accepted: 11 October 2021

5 © The Author(s), under exclusive licence to Springer Nature B.V. 2021

6 Abstract

7 Observation of the variations in the Earth's rotation at time scales ranging from subdi-
8 urnal to multidecadal allows us to learn about its deep interior structure. We review all
9 three types of motion of the Earth's rotation axis: polar motion (PM), length of day varia-
10 tions (Δ LOD) and nutations, with particular attention to how the combination of geodetic,
11 magnetic and gravity observations provides insight into the dynamics of the liquid core,
12 including its interactions with the mantle. Models of the Earth's PM are able to explain
13 most of the observed signal with the exception of the so-called Markowitz wobble. In addi-
14 tion, whereas the quasi-six year oscillations (SYO) observed in both Δ LOD and PM can
15 be explained as the result of Atmosphere, Oceans and Hydrosphere Forcing (AOH) for
16 PM, this is not true for Δ LOD where the subtraction of the AOH leads to an amplified
17 signal. This points to a missing—possibly common—interpretation related to deep interior
18 dynamics, the latter being also the most likely explanation of other oscillations in Δ LOD
19 on interannual timescales. Deep Earth's structure and dynamics also have an impact on
20 the nutations reflected in the values of the Basic Earth Parameters (BEP). We give a brief
21 review of recent works aiming to independently evaluate the BEP and their implications for
22 the study of deep interior dynamics.

23 Article Highlights

- 24 • Review of observations of the three components of Earth's rotation using magnetic,
25 gravimetric and geodetic measurements.
26 • Discussion of the implications for the dynamics of the Earth's liquid core.
27 • Perspective on future theoretical and experimental development.

28 **Keywords** Earth's rotation · Polar motion · Length of day · Nutation · Observation

A1 ✉ Jérémy Rekier
A2 jeremy.rekier@observatory.be

A3 ¹ Royal Observatory of Belgium, Ringlaan 3, BE-1180 Brussels, Belgium

29 1 Introduction

30 Variations in the Earth’s rotation can all be traced back, ultimately, to transfer of angular
 31 momentum, either between the planet and its surrounding—primarily due to the torques
 32 exerted by the Sun and Moon—or among the internal layers within the planet itself.

33 1.1 The Three Components of Earth’s Rotation

34 When talking about variations in rotation, we mean either the changes in the magnitude or
 35 direction of the angular velocity vector of the planet or those in the orientation of the plan-
 36 etary figure itself, the two being related by kinematic relations. Changes in the rotation rate
 37 result in *variations in the length of day* (ΔLOD). Changes in the rotation axis orientation
 38 can be observed as movements of the poles in space. The motion known to astronomers as
 39 the *Precession of equinoxes* is a secular motion of that latter type which takes the Earth’s
 40 pole around the normal to the ecliptic in a period of about 25,700 years. Nutations come in
 41 addition to this secular motion manifesting themselves as a series of oscillations of shorter
 42 periods about the mean equinox. These are, for the most part, caused by the tidal torques
 43 exerted by the Sun and Moon. For historical as well as technical reasons, it is customary to
 44 further separate these oscillations in two kinds based on their frequencies. Roughly speak-
 45 ing, one then speaks of (precession–) *nutations* to denote oscillations that have a low fre-
 46 quency as measured from a *Celestial Reference Frame* (CRF), whereas other kind of oscil-
 47 lations is referred to as the *polar motion* (PM). The latter consists mainly of oscillations of
 48 subdiurnal frequencies as measured in a *Terrestrial Reference Frame* (TRF) (see Dehant
 49 and Mathews (2015) for details).

50 1.2 Reference Frames

51 More specifically, when speaking either of nutations or polar motion, we refer to the
 52 motion of the *Celestial Intermediate Pole* (CIP) with respect to the *International Celestial*
 53 *Reference Frame* (ICRF) or the *International Terrestrial Reference Frame* (ITRF), respec-
 54 tively. The definition of the CIP was adopted by the *International Astronomical Union*
 55 (IAU) in 2000 in order to replace the previous *Celestial Ephemeris Pole* (CEP) and to
 56 accommodate significant improvements in the Earth’s observation. This led to the formal
 57 classification of nutations and PM according to Fig. 1, where nutations are identified as
 58 oscillations of the CIP with frequencies $-0.5 \leq \omega \leq 0.5$ (in cycles per sidereal day, cpsd)

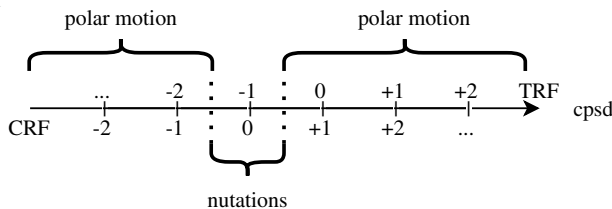


Fig. 1 Conventional definitions of polar motion (PM) and nutations of the CIP. Nutations have frequencies in the interval $-0.5 \leq \omega \leq 0.5$ measured in the Celestial Reference Frame (CRF). PM covers all the remaining corresponding frequencies as they appear in the Terrestrial Reference Frame (TRF). The difference of 1 cycle per sidereal day (cpsd) between the two frames corresponds to the diurnal rotation rate of the Earth

59 as measured from the ICRF, whereas PM are oscillations of the CIP with frequencies in
60 the intervals $-\infty < \omega \leq -0.5$ and $0.5 \leq \omega < \infty$ in the ITRF. As there is a difference of +1
61 cpsd when going from the ITRF to the ICRF (accounting for the diurnal rotation of the
62 Earth), wobbles of the instantaneous rotation axis with frequencies within the interval -1.5
63 to -0.5 cpsd (*i.e.* with periods close to either $2/3$ or 2 sidereal days corresponding to ~ 15.9 h
64 and ~ 47.9 h, respectively) are equivalent to nutations. Note that one speaks about wobble
65 instead of PM in this case as PM is a term classically used for the CIP motion in the TRF.

66 As the Earth's rotation is very close to a steady state, it is customary to write the rota-
67 tion vector as:

$$\Omega = \Omega_0(\hat{\mathbf{z}} + \mathbf{m}), \quad (1)$$

68 where we have chosen the Cartesian basis vector, $\hat{\mathbf{z}}$, in the direction of the mean spin-axis.
69 $\Omega_0 = 1$ cpsd denotes the mean angular rate of rotation, and the vector \mathbf{m} is called the plane-
70 tary *wobble*. This last quantity is typically very small with a magnitude of the order of 10^{-8}
71 to 10^{-6} for the Earth. For this reason, the equations of conservation of angular momentum
72 governing the time evolution of \mathbf{m} can be safely restricted to first order. This effectively
73 decouples the axial component of rotation m^z from the equatorial components m^x and m^y
74 where the Cartesian geographical x coordinate points to the Greenwich Meridian and the
75 y coordinate points to the 90° East longitude. Classically, one then uses the term 'wob-
76 ble' in relation to the latter two components exclusively. The dynamics of m^z models the
77 modulations in the LOD while m^x and m^y model both PM and nutations expressed in the
78 TRF. Quantitatively, ΔLOD does not exceed a few milliseconds (ms), typical PM is of the
79 order of several hundreds of milliarcseconds (mas) (corresponding to a PM within a square
80 of 20 m side), and the dominant component of nutations (Bradley's nutation of 18.6-year
81 period) has an amplitude of about ± 19 arcsec and ± 10 arcsec in longitude and obliquity,
82 respectively. The wobble corresponding to nutations is of the order of several milliarcsec-
83 onds (mas).
84
85

86 1.3 Origins of the Earth's Movement

87 Broadly speaking, PM is typically associated with variations in the orientation of the rota-
88 tion axis caused by geophysical processes, *i.e.* the redistribution of the masses inside the
89 Earth that gets reflected in the inertia tensor. Such redistributions result in both secular and
90 oscillatory variations. On the other hand, nutations are more affected by torques resulting
91 from the tidal forces from external sources (primarily the Moon and Sun). This distinc-
92 tion is, however, a matter of nomenclature. For example, in reality, excitations from outer
93 sources do also cause redistributions of masses inside the Earth (Mathews and Bretagnon
94 2003). For our purpose, the two types of motions can nevertheless be clearly separated on
95 the basis of observation.

96 Conventionally in geodesy, studies of PM (including wobble) and nutations assume
97 that the flow inside the core has a uniform vorticity, *i.e.* it resembles a solid-body rotation
98 around an axis forming a finite angle with the mantle's rotation. It can be shown that the
99 core flow bears little effect on the excitation of PM (see *e.g.* Chap. 7 of Bizouard 2020).
100 However, as explained in Sect. 2 the mere presence of the fluid core affects the PM by
101 altering the frequency of the free rotational mode known as *Chandler Wobble* (CW)—and
102 to a lesser extent the *Inner Core Wobble* (ICW) (see later). Nutations, on the other hand,
103 are directly affected by the core flow, and so their study offers a window on a broad variety
104 of physical processes taking place inside the fluid core as reviewed in Sect. 4. The fluid

105 core also has an indirect effect on the frequencies of the free rotational modes known as the
106 *Free Core Nutation* (FCN) and *Free Inner Core Nutation* (FICN) that manifest themselves
107 as resonances in the forced nutation series. The FCN also appears in the nutation series at
108 its own free frequency excited by the continual forcing attributed mostly to the atmosphere
109 and oceans. Once deconvolved from the excitation signal, the frequency of this mode pro-
110 vides valuable information about the core (Chao and Hsieh 2015).

111 Whereas the functional definitions of PM and nutation allow a clear distinction based on
112 the frequencies as stated above, such a distinction does not exist for LOD. Δ LOD contains
113 a broad variety of timescales. In addition to a secular trend, which can be attributed to
114 the luni-solar tidal frictions (Munk and MacDonald 1960) plus contributions from Glacial
115 Isostatic Adjustment (GIA, see later) and tectonic forces (Gross 2015), the total Δ LOD
116 signal contains many oscillations with timescales ranging from decadal, interannual, intra-
117 seasonal, diurnal, and up to subdiurnal. Diurnal and subdiurnal oscillations are attributed
118 to tides (Defraigne and Smits 1999). Oscillations at the interannual, seasonal, and inter-
119 seasonal timescales have been satisfactorily attributed to the exchange of angular momen-
120 tum between the solid Earth and its fluid envelope (*i.e.* atmosphere and oceans) (Viron
121 et al. 1999, 2001) while earthquakes have surely induced relatively small changes (see *e.g.*
122 Gross and Chao 2006). Although not directly related to rotation, it has been pointed out
123 that the *Slichter modes* with theoretical frequencies of the same order as the subdiurnal PM
124 (as measured in the TRF) might be detectable in the gravimetric signal which calls for cau-
125 tion in interpreting the data (Rosat and Hinderer 2018).

126 1.4 Implications for the Deep Earth's Dynamics

127 Of more interest to this review's purpose are the decadal and interannual oscillations in the
128 LOD, the amplitudes of which have been proven too large to be attributed to the atmos-
129 phere and oceans solely, thus hinting towards the probable implication of deep interior
130 dynamics, where the core motions are the obvious culprit. In fact, the correlation between
131 the variations in the Earth's magnetic field and the length-of-day variations at decadal
132 timescales (Ball et al. 1969) suggests that the core motions inducing the variations in the
133 magnetic field generate a pressure field at the core–mantle boundary (CMB) causing in
134 turn a change in the Earth's rotation (Hide 1969). Jault et al. (1988) demonstrated that both
135 the frequencies and amplitudes of these Δ LOD fluctuations can be largely explained by the
136 excitation of torsional oscillations, time-variable oscillations in the core flow in the form of
137 coaxial Taylor cylinders around the figure axis which oscillate with a particular period of
138 several years (6 years is typically considered). A more detailed theoretical account of this
139 type of oscillations is given in Triana et al., this issue. The most important implications for
140 our purpose are given in Sect. 3. The existence of the torsional oscillations warrants the
141 close measurement of the decadal Δ LOD.

142 We thus see how PM, nutations and Δ LOD observations are complementary when
143 examining the nature and dynamics of the flow inside the Earth's core at various time-
144 scales. In the remainder to this chapter, we turn to each of these motions and review the
145 techniques used for their modelling and observations before discussing the fluid core
146 dynamics. Section 5 concludes with perspectives on future work.

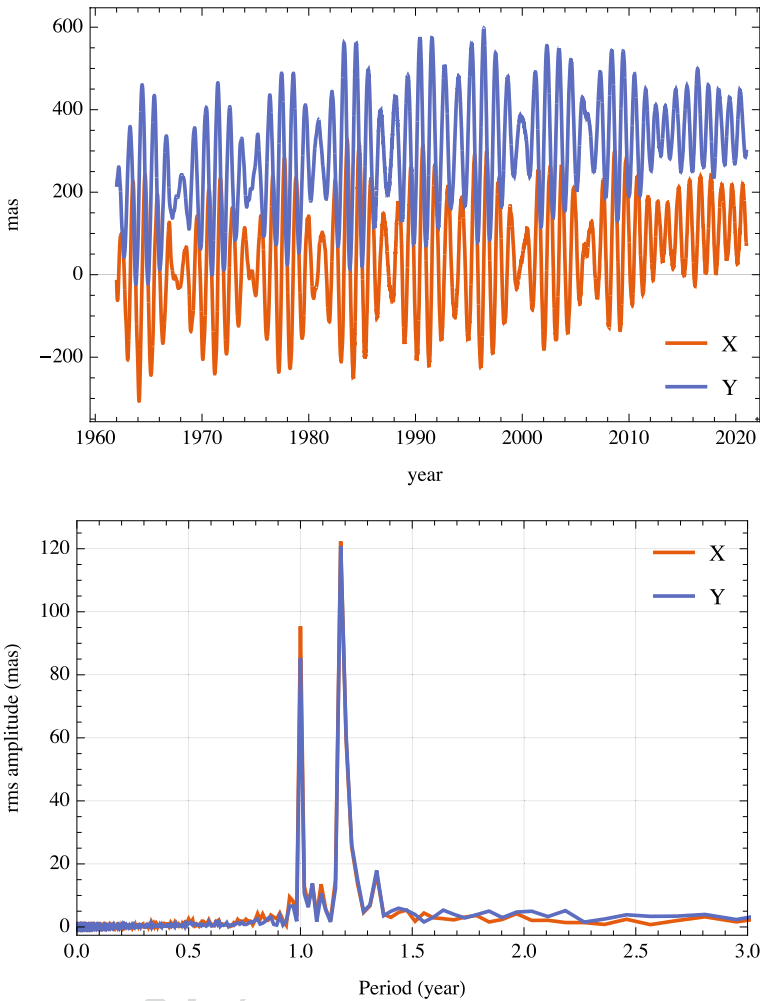


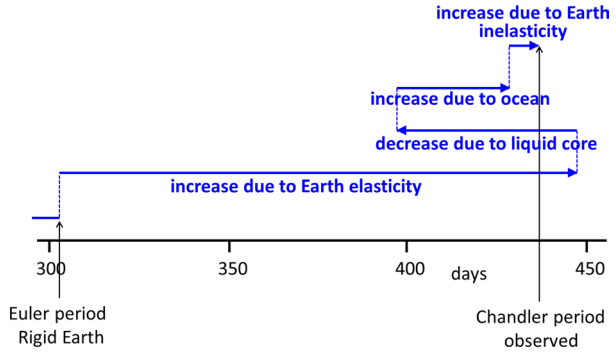
Fig. 2 Polar motion coordinates X and Y, where X is defined towards Greenwich and Y towards 90 degree East as determined by VLBI and Global Navigation Satellite Systems (GNSS) techniques (EOP Combined Serie C04, see details at [IERS](#))

147 **2 Polar Motion**

148 **2.1 Modelling and Observations**

149 Polar motion (PM) is the motion of the mean rotation axis (more precisely of the CIP—see
 150 Sect. 1) around the symmetry axis of the Earth measured in the TRF. The upper panel of
 151 Fig. 2 shows the two components, X and Y, of this motion for the past six decades based on
 152 the EOP Combined Serie C04 (see [IERS](#)). The signal has two dominant frequency compo-
 153 nents, as can be observed from the bottom panel representing its simple Fourier Transform.
 154 One of the peaks is at the period of one year, the other corresponds to a period of about
 155 432 days in the TRF. The annual wobble is due to the forcing by surface fluid layers. The

Fig. 3 Period of the CW is altered by a series of geophysical processes



156 432 days resonance is due to the CW which is the Earth’s analog to the *Eulerian nutation*
 157 for a rigid ellipsoidal body (Bizouard 2020).

158 The CW is excited mainly by the atmosphere, the oceans and to a lesser extent by
 159 hydrological masses through the afore-mentioned exchange of angular momenta. In
 160 practice, geophysical excitation functions are provided by services to the geodesy com-
 161 munity (IERS) based on data assimilation and numerical models of the atmosphere and
 162 ocean, considering that the oceans are responding dynamically to the atmospheric pressure
 163 changes (see e.g. Bizouard 2020, for details).

164 The CW is a rotational normal mode whose frequency depends directly on the dynamic
 165 oblateness of the Earth modified by the planet’s interior structure and feedback from the
 166 CW deformation itself (Munk and MacDonald 1960). Mathematically, for an elastic ellip-
 167 soidal axisymmetric Earth’s model, the CW frequency writes:

168
$$\sigma_{CW} = \left(1 - \frac{k_2}{k_s} \right) \sigma_e, \tag{2}$$

169 where $\sigma_e = \Omega_0(C - A)/A$ is the Eulerian nutation of period 304.5 sidereal days (or 303.6
 170 mean solar days) and $k_2 = 0.302$ and $k_s = 0.942$ are the degree-2 and secular Love num-
 171 bers that characterize the Earth’s elastic and anelastic deformability.

172 If the oblate Earth were rigid, the period of the CW would be equal to the Eulerian
 173 period of ~ 305 sidereal days. The Earth having an inelastic mantle, a liquid core, an inelas-
 174 tic inner core, and oceans, this period is in reality about 432 days. These different contribu-
 175 tions are shown in Fig. 3, where we see that the presence of a liquid core decreases the CW
 176 period by about 40 days. Physically, the CW can be excited by external torques inducing an
 177 angle between the principal moment of inertia and the Earth’s figure axis or when a large
 178 mass redistribution or surface deformation alters the inertia tensor of the Earth, the lat-
 179 ter mechanism being the most prominent. The presence of a liquid core changes the mass
 180 involved in the mechanism. Mathematically, the CW period will be proportional to the
 181 mantle moment of inertia instead of the whole Earth moment of inertia in Eq. (2) when the
 182 liquid core does not participate in the motion at the timescale under consideration, reduc-
 183 ing the CW period accordingly.

184 In addition to the CW, the presence of an ellipsoidal inner core introduces another rota-
 185 tional normal mode which can, in principle, become excited when there is a finite angle
 186 between the rotation and figure axes of the inner core. This is the ICW introduced in Sect. 1
 187 and is analogous to the CW for the oblate inner core. The moment of inertia of the inner
 188 core is 1400 times smaller than the whole Earth’s, and its dynamical oblateness is also
 189

190 comparatively smaller. Consequently, the frequency of the ICW is presumably much lower
191 than that of the CW. Additionally, if excited, the ICW would have to transmit its angular
192 momentum to the mantle somehow (e.g. via gravitational torque) in order to observe its
193 contribution to polar motion. So far no firm evidence of the ICW within a resolution of
194 a few mas has been found. A spectral search in PM by Guo et al. (2005) showed that the
195 gravitational perturbation induced by the ICW would be far below the detectability level of
196 current ground (e.g. superconducting gravimeters) and space (e.g. GRACE) gravity meas-
197 urements. More recently, a 8.7-yr peak detected in PM time-series was suggested to be pos-
198 sibly related to the ICW (Ding et al. 2019), although most of the long-period polar motion,
199 except for the Markowitz period (see below), is generally considered to be attributable to
200 climatological signals.

201 Beyond the 10-year period, PM is dominated by a 25–35- year pluri-decennial oscilla-
202 tion with a mean amplitude as large as 10 mas. This is the so-called *Markowitz wobble*
203 (Markowitz 1960, 1961). The coupling between core and mantle is believed to be insuf-
204 ficient to explain that term (Hide et al. 1996). As the associated observation errors were too
205 large to definitely conclude about it prior to the use of space geodesy, longer and more pre-
206 cise geodetic time-series should help to further characterize the Markowitz wobble. Centi-
207 metre accuracy in the realization of the TRF and of PM is possible thanks to an increasing
208 precision of the space-geodetic observations but necessitates to take into account tectonic
209 plate motions. Considering this and imposing the minimum rotation of the plates as a
210 prepositional condition for the TRF, it is possible to see that the rotation pole has shifted
211 by over 10 meters (about 300 mas) since first defined in 1900. This secular PM is mostly
212 attributed to the *Glacial Isostatic Adjustment* (GIA) modified by present-day ice melting
213 (Adhikari and Ivins 2016) and slightly by large earthquakes (Xu and Chao 2019) in recent
214 years (see below).

215 In addition to the above-mentioned components, PM signal also contains shorter time-
216 scales that correlate with changes in the angular momenta of the atmosphere, ocean and
217 hydrosphere and earthquake. By virtue of the definition of the TRF and CRF evoked in
218 the introduction to this work, the retrograde diurnal motions are equivalent to the wobble
219 associated with nutation. This includes a *Nearly Diurnal Free Wobble* (NDFW) which is
220 perfectly equivalent to the FCN but expressed in the TRF. However, the retrograde diurnal
221 wobble motion is observed as a long-term CIP motion in the CRF including an excitation
222 of the FCN (Bizouard et al. 2019).

223 2.2 Interpretation

224 The observed PM is the convolution of the Chandler Wobble resonance with the geophysi-
225 cal excitation function representing Atmospheric, Oceans and Hydrosphere Forcing (AOH)
226 (Munk and MacDonald 1960). The PM excitation function can hence be obtained through
227 a deconvolution procedure (see e.g. Chao 1985). Its two equatorial components, designated
228 as PM-X and PM-Y, are both characterized by a significant long-term variability on top of
229 strong seasonal and intraseasonal variations (see comparisons in Fig. 4). The seasonal vari-
230 ability in PM-Y is notably larger than that of PM-X. This is attributed to the geographical
231 distribution of major continents which are more aligned in the Y axis and produce relatively
232 larger excitation of PM-Y from atmospheric surface pressure loading and terrestrial water
233 storage changes, whereas atmospheric loading effect over the oceans is largely compen-
234 sated by the inverted barometer response of the ocean surface. The long-term variability
235 of PM-X and -Y is presumably mainly excited by solid Earth geophysical effects, e.g. GIA

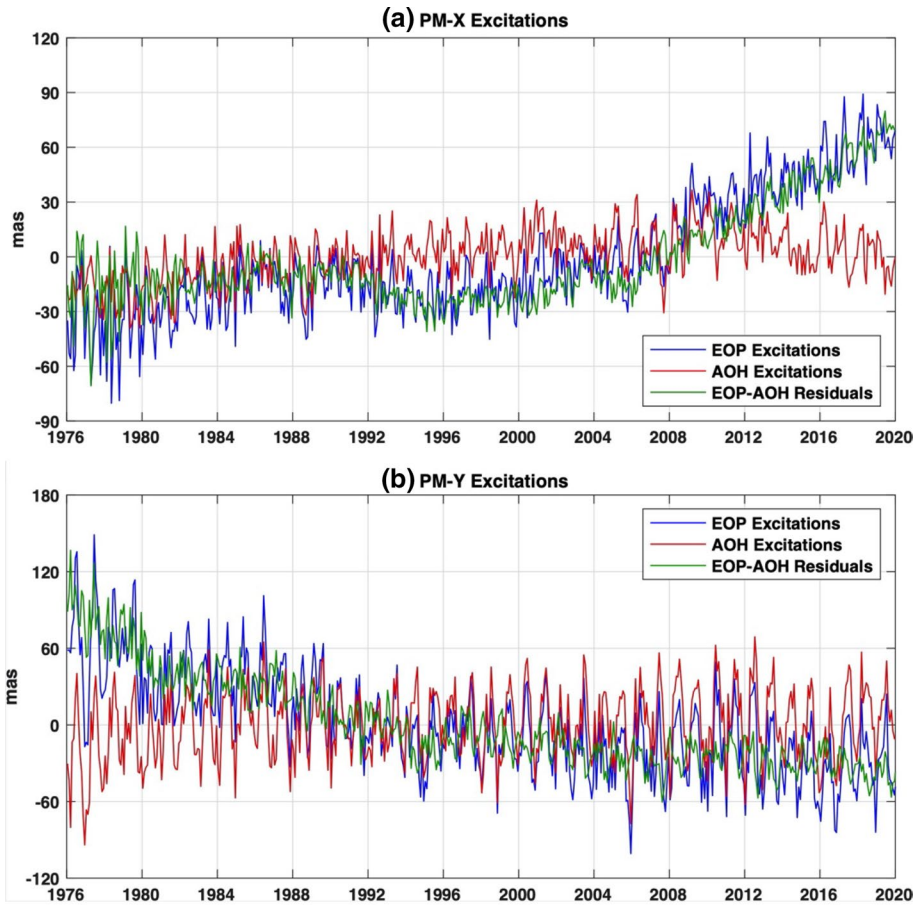


Fig. 4 Deconvolved monthly excitations of the observed polar motion: (a) PM-X and (b) PM-Y, from the IERS EOP C04 series and compared geophysical excitations from AOH (the sum of atmospheric, oceanic, and hydrological contributions) over the period 1976–2019. The AOH series are from the GFZ EAM products. EOP-AOH residuals are shown in green curves for comparisons

236 (Peltier 2004). At decadal and longer time scales, mass loss in polar ice sheets and glaciers
237 and corresponding sea level changes are found to play a fairly important role in exciting
238 PM as well (Chen et al. 2013; Adhikari and Ivins 2016).

239 While broad-band decadal variability, other than the Markowitz wobble, is not so evi-
240 dent in PM excitation (as compared to Δ LOD, see Sect. 3), PM-X and -Y do exhibit clear
241 interannual oscillations. Comprehensive analysis of interannual oscillations in PM excita-
242 tion and AOH geophysical excitations has been carried out to identify periodic interan-
243 nual oscillations in both components (Chen et al. 2019). The AOH excitations are from the
244 effective angular momentum (EAM) products provided by the German GeoforschungsZe-
245 ntrum (GFZ) (Dobslaw and Dill 2018). The daily EOP C04 and 3-hourly EAM series have
246 been averaged into monthly intervals. Large uncertainties in EAM series are expected,
247 especially in the hydrological components due to the immaturity of hydrological models.
248 PM-X shows a clear oscillation near 5.9 years, plus smaller variations at shorter periods.
249 Atmospheric, Ocean and Hydrosphere (AOH) sources largely account for the 2.5–and

250 3.65-year components found in PM-Y. It is interesting to note that AOH excitations also
251 show notable quasi six-year oscillation (SYO) signals in both PM-X and -Y that are mostly
252 in phase with *Earth's Orientation Parameters* (EOP) Combined Serie C04 (see [IERS](#) for
253 details). After AOH excitations are removed, the SYO in PM becomes even less notable
254 so that it is not possible at present to conclude that this SYO in PM, if present, is caused
255 by core processes (Rosat et al. 2020). This is contrary to the case with the SYO in Δ LOD
256 where the SYOs in Δ LOD and AOH are out of phase, and removing AOH makes the SYO
257 in Δ LOD appear more clearly (see Sect. 3).

258 The quantification of the SYO in PM is more difficult due to the small magnitudes of
259 the signal (compared to seasonal variability) and existence of other interannual oscillations
260 more clearly related to AOH sources. The main challenges in quantifying the SYO in PM,
261 especially the variation related to the solid Earth, include how to improve the quantification
262 of SYO amplitudes and phases in both PM observations and the atmospheric, oceanic and
263 hydrological AOH model predictions. The latter may play a more important role, as the
264 uncertainties of atmospheric, oceanic and hydrological model predictions (including mass
265 and motion terms) appear to be the major limitations affecting the appropriate separation of
266 any SYO signals that might be related to core-mantle interactions (Chen et al. 2019). The
267 magnitudes of the SYO in PM appear to also depend strongly on time spans of the EOP
268 time series. Nevertheless, further investigation of interannual oscillations in PM from both
269 EOP observations and AOH sources is needed.

270 At multi-decadal time scales, AOH excitations of PM can only be determined from
271 atmospheric, oceanic and hydrological model predictions due to inadequate *in situ* obser-
272 vations. Among the three major components of the climate system, the largest uncertainty
273 appears to come from model-based estimates of terrestrial water storage (TWS) change
274 (Chen and Wilson 2005; Nastula et al. 2019), although it has long been recognized that
275 global TWS change plays an important role in exciting PM at seasonal and interannual
276 time scales (Chen et al. 2000; Nastula et al. 2007).

277 Another important feature of PM is its attenuation with time due to dissipative pro-
278 cesses. Dissipation occurs through anelastic deformation in the mantle, viscomagnetic
279 coupling at the core-mantle boundary, friction at the bottom of the oceans, etc. Dissipa-
280 tion is quantified by a quality factor, Q , that may be related to the rheological parameters.
281 The determination of Q at the CW frequency, which again requires a Chandler resonance
282 deconvolution, thus provides additional constraints on the Earth rheology at frequencies
283 intermediate between seismic and tidal frequencies (Benjamin et al. 2006).

284 The movement of the Earth's rotation axis induces a perturbation of the surface gravity
285 field through variation in the centrifugal potential, surface deformation and mass redistri-
286 bution. These changes have been analysed from superconducting gravimeter (SG) measure-
287 ments longer than a decade by Ziegler et al. (2016a). In particular, assuming some given
288 rheological models for the Earth's mantle the link between the gravimetric factor phase and
289 the CW quality factor could be made (Ziegler et al. 2016a, b). However, one would need
290 data sets spanning at least 31 years to obtain stable estimates of the CW damping (Gross
291 2015).

292 At decadal time-scales, the exchange of angular momentum between the fluid outer core
293 and solid mantle was long thought to be responsible for the observed decadal PM. How-
294 ever, the electro-magnetic (EM) torque computed from geomagnetic observations at the
295 Earth's surface is too weak to explain the observed decadal PM. Notwithstanding, Kuang
296 et al. (2019) have recently simulated the toroidal magnetic field in the D'' -layer from the
297 induction and convection of the toroidal field in the outer core showing that it could be
298 much stronger than that from the advection of the poloidal field in the outer core. This

reassessment of EM coupling using dynamo simulations shows that it could still contribute largely to decadal PM to magnitude of approximately 10 mas.

Besides CW, measurements of the ICW period would provide a valuable fundamental constraint on the deep Earth's properties. Theoretical estimates based on the conservation of angular momentum and the PREM model of interior predict a period of about 7.5 years prograde. The indirect (resonance) effect of the ICW on nutations hints to a somewhat smaller period of about 2400 days (Mathews et al. 2002b). Ding et al. (2019) have recently showed how the ICW detection could provide a new independent constraint on the density contrast at the ICB. If the detected signal in PM data at 8.7-yr is the signature of the ICW, then it would imply a density contrast of $\sim 507 \text{ kg/m}^3$ (Ding et al. 2019). Such a value is smaller than the 600 kg/m^3 for PREM model (see Dehant et al., this issue).

3 Δ LOD

3.1 Modelling and Observations

The best way to measure Δ LOD precisely is by using *Very Long Baseline Interferometry* (VLBI). This technique consists of observing light emitted by radio-sources in S- or X-bands using large antennas on Earth of typically 25 m diameter. The arrival time of the signal at two different stations is then used to compute the (time varying) time delays and infer the Earth orientation relative to the celestial radio-sources taken as stationary (or with a small proper motion characterized *a priori*). After correcting for the time delays induced by atmospheric and other miscellaneous environmental effects, it is possible to derive UT1-UTC, a quantity directly related to the Earth rotation angle with respect to the mean Earth rotation by using a large network of stations and radio-sources (Fey et al. 2015). Information on Δ LOD may then be recovered from:

$$\frac{\Delta\text{LOD}(t)}{\Omega_0} = \frac{d(\text{UT1} - \text{TAI})}{dt}, \quad (3)$$

where $\Delta\text{LOD}(t)$ is called the *excess of length of day*, $\Omega_0 = 86400s$ is the mean rotation rate of Earth, UT1 is the Universal Time and TAI is the reference International Atomic Time (related to UTC—Coordinated Universal Time—by a set of leap seconds). VLBI is the only method that can access the absolute UT1 information. It is classically determined weekly by the *International VLBI Service* (IVS) R1 and R4 sessions with an error of the order of $2 - 3 \mu s$ (microsecond), as well as via daily one-hour intensive sessions at the level of $\sim 20 \mu s$ accuracy (Malkin 2020).

Δ LOD takes place on all observable time scales, from subdaily to decadal and beyond (see Fig. 5). It is due to angular momentum changes of the solid Earth in two forms: mass redistribution and the relative motion of the atmosphere, ocean, and the liquid outer core. Tidal forces, primarily from the Sun and Moon, cause Δ LOD through the deformation that they induce on the Earth's mass distribution. These effects are observed using high accuracy space geodetic measurements system (Schuh and Behrend 2012). The periods of the principal zonal tidal components are mostly at the intra-annual timescale with a few notable exception such as the 'regression of the lunar nodes' (*a.k.a.* lunar precession) which has a period of 18.6 years. Table 1 reproduces the 20 tidal components that have the largest effect on Δ LOD (Ray and Erofeeva 2014).

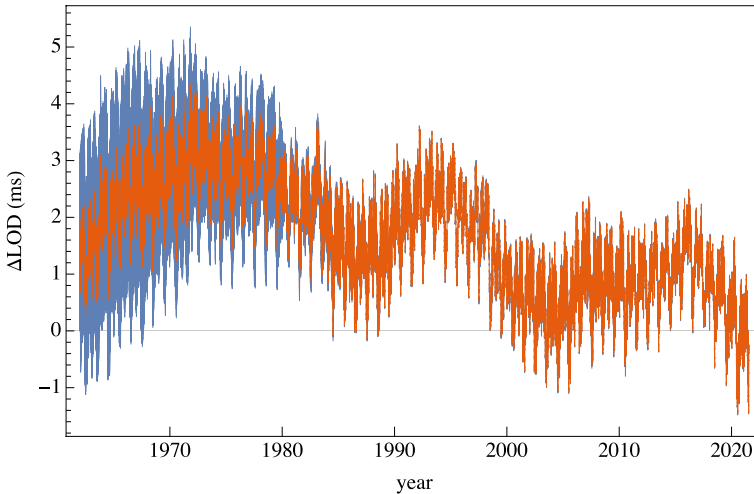


Fig. 5 Δ LOD as measured with VLBI and Global Navigation Satellite Systems (GNSS) techniques (Combined Serie C04, see [IERS](#) for details) with uncertainties in blue. Δ LOD contains a rich spectrum of information covering periods from days to multidecadal. It can be partly explained by the mass redistribution or the motion of the atmosphere, the hydrosphere, and the core

341 The redistribution of masses due to atmospheric, oceanic and hydrological excita-
342 tions also alter Earth's angular momentum causing Δ LOD at seasonal and interannual
343 timescales. Numerical models computing the angular momentum attributed to meteoro-
344 logical processes have improved significantly in recent years reaching a time resolution
345 of three hours in the evaluation of atmospheric (AAM), oceanic (OAM) and hydrologic
346 (HAM) angular momentum (Dobslaw and Dill 2018). Gross et al. (2004) showed that
347 AAM explains 85.8% of Δ LOD variations at the interannual time scale, but that taking
348 into account OAM and HAM contributions only offers a marginal improvement. In addition,
349 climatic oscillations most likely play a role in Δ LOD. A high correlation was found,
350 for example, between Δ LOD, the El Niño–Southern Oscillation (ENSO) and the quasi-
351 biennial oscillation (Chao 1989).

352 In addition to the oscillatory components mentioned above, a much longer secular vari-
353 ation is partly attributed to the deceleration caused by tidal frictions in the Earth–Moon
354 system (Munk 1997). The linear regression fitting of ancient Δ LOD observations going
355 back to 4000 years ago based on lunar and solar eclipses records by Babylonian, Chinese,
356 Greek and Arab astronomers predicts a +1.8 ms/cy per century increase in Δ LOD. This is,
357 however, contrasting with the +2.3 ms/cy predicted by tidal friction alone (see Fig. 6) leav-
358 ing an unexplained gap of about +0.7 ms/cy. Part of this gap is at least partly explicable as
359 the result of the GIA inside the Earth (Mitrovica et al. 2015), a process through which the
360 figure (and the inertia tensor) of the Earth is altered by deglaciation. Models suggest that
361 GIA-induced Δ LOD is very sensitive to the assumed value of lower mantle viscosity (Wu
362 and Peltier 1984; Peltier and Jiang 1996; Peltier 2007) as well as to changes in the mass of
363 glaciers and ice sheets. The Antarctic ice sheet melting-induced mass changes could lead to
364 a -0.72 ms/cy to $+0.31$ ms/cy in Δ LOD according to Ivins and James (2005). In addition,
365 the subsurface tectonic activities (Van der Wal et al. 2004), earthquakes (Chao and Gross
366 1987), plate subduction, deformation of the mantle and core–mantle interactions, etc. could

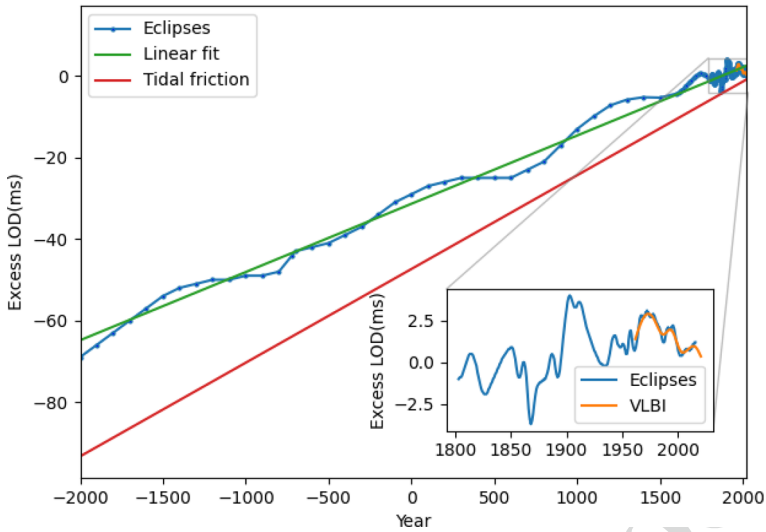


Fig. 6 Secular change in the LOD from 2000 B.C. to present day based on Stephenson et al. (2016). The historical Δ LOD change is estimated from past lunar and solar eclipses documented by Babylonian, Chinese, Greek and Arab astronomers. The linear regression shows a +1.6 ms/cy in Δ LOD with time, which is 0.7 ms/cy lower than the decrease in Earth’s rotation rate (+2.3 ms/cy) predicted by tidal friction alone

Table 1 Twenty major zonal tidal components in Δ LOD (reproduced from Ray and Erofeeva (2014))

| Period (days) | V_0/g (cm) | UT(cos) (μ s) | UT(sin) (μ s) | LOD(cos) (μ s) | LOD(sin) (μ s) |
|---------------|--------------|--------------------|--------------------|---------------------|---------------------|
| 6798.405 | 2.79288 | 1764.00 | -172958.94 | 159.851 | 1.630 |
| 3399.202 | 0.02726 | 8.46 | -840.24 | 1.553 | 0.016 |
| 1305.483 | 0.00379 | 0.47 | -44.55 | 0.214 | 0.002 |
| 1095.178 | 0.00145 | 0.15 | -14.35 | 0.082 | 0.001 |
| 385.998 | 0.00420 | 0.19 | -14.53 | 0.236 | 0.003 |
| 365.259 | 0.49215 | 20.78 | -1608.33 | 27.666 | 0.358 |
| 346.636 | 0.00311 | 0.13 | -9.64 | 0.175 | 0.002 |
| 182.621 | 3.09884 | 71.94 | -5042.06 | 173.475 | 2.475 |
| 121.749 | 0.18092 | 3.20 | -195.78 | 10.104 | 0.165 |
| 31.812 | 0.67279 | 6.78 | -187.98 | 37.128 | 1.339 |
| 27.555 | 3.51840 | 33.91 | -849.42 | 193.690 | 7.731 |
| 23.942 | 0.04912 | 0.45 | -10.27 | 2.696 | 0.119 |
| 14.765 | 0.58366 | 4.48 | -74.13 | 31.545 | 1.908 |
| 13.777 | 0.28836 | 2.15 | -34.07 | 15.536 | 0.978 |
| 13.661 | 6.66068 | 49.36 | -779.88 | 358.699 | 22.702 |
| 9.557 | 0.24217 | 1.447 | -19.417 | 12.766 | 0.952 |
| 9.133 | 1.27531 | 7.367 | -97.403 | 67.010 | 5.068 |
| 9.121 | 0.52856 | 3.050 | -40.311 | 27.770 | 2.101 |
| 7.096 | 0.20369 | 0.940 | -11.869 | 10.509 | 0.832 |
| 6.859 | 0.16872 | 0.751 | -9.480 | 8.684 | 0.688 |

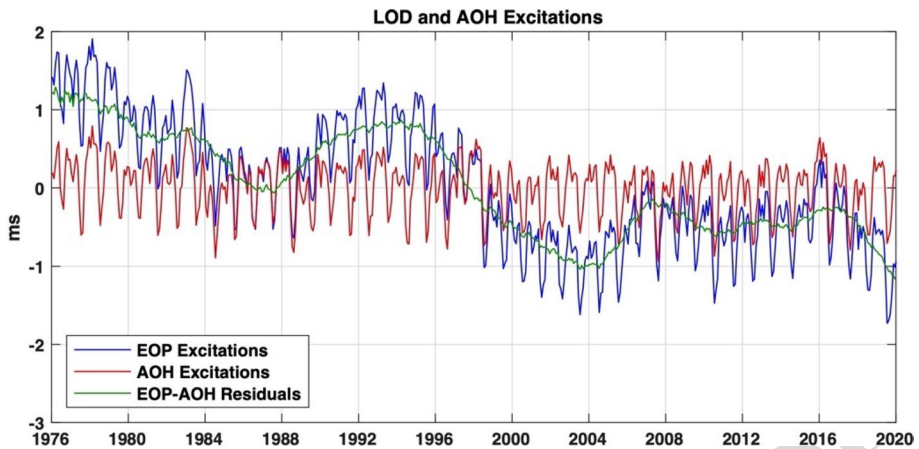


Fig. 7 Comparisons of observed monthly LOD excitations from the IERS EOP C04 series and geophysical excitations from AOH (the sum of atmospheric, oceanic, and hydrological contributions) over the period 1976-2019. The AOH series are from the GFZ EAM products (covering the period 1976 onward)

367 also alter Δ LOD (Dumberry and Bloxham 2006; Holme 1998; Jault and Le Mouél 1990;
368 Mound and Buffett 2003).

369 3.2 Interpretation

370 AAM changes have long been recognized as dominantly driving Δ LOD, accounting for
371 $\sim 90\%$ of LOD variations at seasonal and shorter time scales (Rosen and Salstein 1983;
372 Barnes et al. 1983). This is clearly illustrated in the comparisons (shown in Fig. 7) of
373 observed Δ LOD excitations derived from the IERS EOP C04 series and total geophysical
374 excitations from the atmospheric, oceanic, and hydrological contributions (noted as AOH).
375 The strong decadal and long-term variability in LOD is likely driven by mass movement in
376 the interior of Earth and angular momentum exchange between the core and mantle (Jault
377 et al. 1988; Hide et al. 1993; Buffett 1996; Mound and Buffett 2006).

378 In addition, a quasi-SYO at period of ~ 5.9 -year has also been observed in Δ LOD,
379 which could not be attributed to either AAM excitation because of different amplitude and
380 phase (see Fig. 8 and Chen et al. 2019) or to other sources in the surface geophysical fluids
381 system (Abarca del Rio et al. 2000; Chao and Hsieh 2015). Indeed, after removing AOH
382 excitations, the amplitude of the SYO becomes more prominent in the LOD residuals and
383 can be better isolated, as can be seen by comparing the black and red curves in Fig. 8.

384 This is shown in Fig. 9 showing the time evolution of the LOD power spectrum in the
385 past 4 decades. The SYO indicated by the lower dashed horizontal line is clearly visible.

386 The remarkable stability of the observed SYO in Δ LOD hints towards a dynamical deep
387 Earth origin (Chao et al. 2014). It is difficult to explain the nearly out of phase SYO in
388 AOH and its dynamical connection with the SYO in observed LOD. It is unlikely to be
389 attributable to errors in the AOH LOD excitations, as similar SYO is also captured in AOH
390 PM excitations, indicating the existence of SYO in the climate system. Further investiga-
391 tions are needed. The quantification of the SYO is also affected by co-existences of other
392 interannual oscillations, in particular a reported 4.9-year (Chen et al. 2019), 8.3-year (Duan
393 and Huang 2020) and 7.3-year (Hsu et al. 2021) oscillation in Δ LOD observations. While

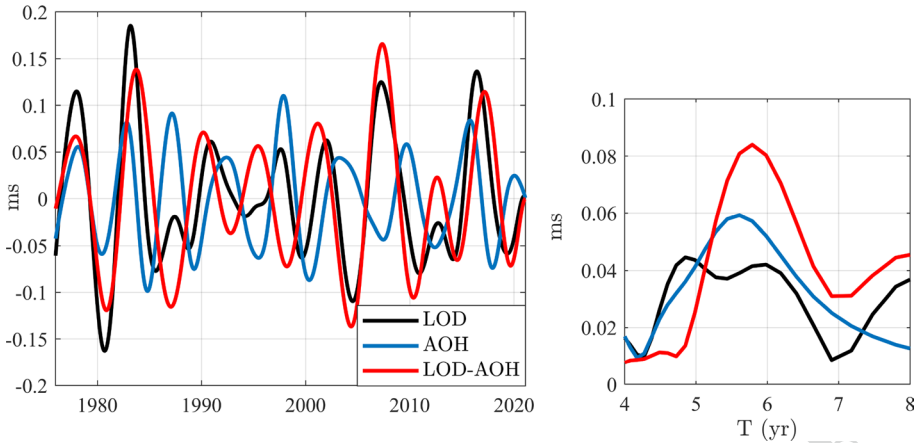


Fig. 8 Observed Δ LOD (only zonal tides were removed), AOH series from the GFZ EAM products and Δ LOD residuals after AOH products were removed. (left) Time-series that were band-pass filtered between 4 and 8 years; (right) amplitude Fourier spectra in ms with respect to period, T , in years

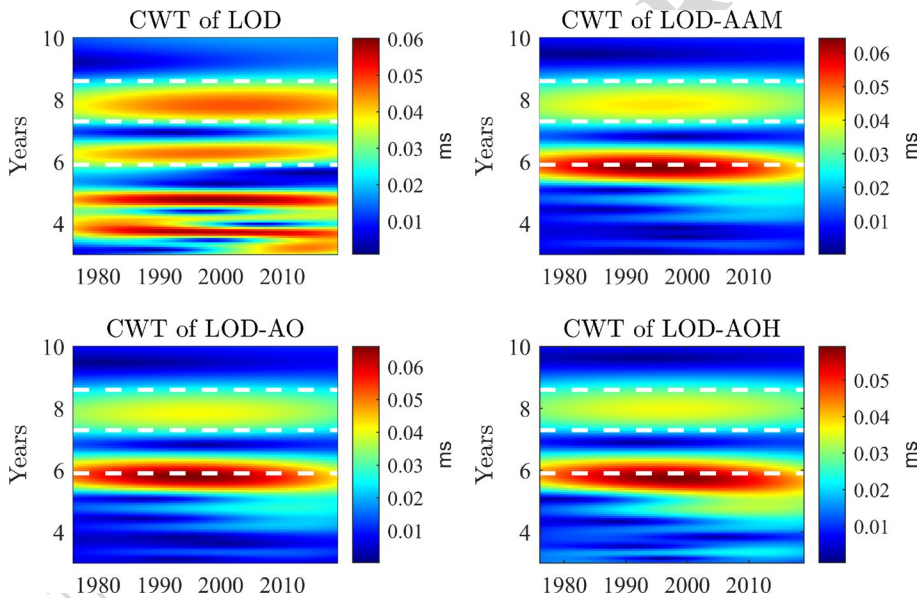


Fig. 9 Continuous Wavelet Transform (CWT) of the LOD signal (upper-left) and the same thing with the contribution from AAM removed (upper-right). Removal of the Oceanic (OAM) and Hydrosphere (HAM) contributions have comparatively small effect on the remaining signal (bottom panels). The horizontal dashed lines correspond to 5.9, 7, and 8.5 years

394 the 4.9-year oscillation is largely accounted for by AAM (Duan et al. 2015), a possible core
 395 origin was suggested for the 8.3 and 7.3-year signals. An extended long record of LOD
 396 series is necessary in order to successfully separate these interannual oscillations with
 397 close-by periods in Δ LOD (see Fig. 8).

398 At least two hypotheses have been proposed treating SYO as a rotational normal mode:
399 the Mantle–Inner-Core Gravitational coupling (MICG) (Buffett 1996; Mound and Buffett
400 2006; Chao 2017; Ding and Chao 2018; Chao and Yu 2020) and the torsional mode in the
401 fluid outer core (Buffett et al. 2009; Gillet et al. 2010), while certain mechanisms have been
402 postulated for the excitation of the mode (see *e.g.* Gillet et al. 2010; Silva et al. 2012; Holme
403 and De Viron 2013). Indeed, the SYO was reported to be correlated with the observed geo-
404 magnetic jerks (Bloxham and Jackson 1991) although their remain some open questions
405 and doubt regarding the exact physical nature of this correlation (Ding et al. 2021). Jerks
406 appear at several locations on a time-scale of a few months as sharp V-shaped features in
407 graphs of magnetic field changes (Mandea et al. 2010). A definite physical model is still
408 lacking at the moment to explain their appearance on the global scale. These might be the
409 result of magneto-hydrodynamic waves causing sharp changes in the flow (Aubert and Fin-
410 lay 2019). Jerks might also be related to the presence of torsional oscillations in the liquid
411 core.

412 The MICG mechanism, on the other hand, has been the subject of debate because of the
413 amplitude of the strength required to transfer angular momentum between core and mantle
414 through gravitational coupling associated with the inner-core superrotation (Davies et al.
415 2014). Chao (2017) has further developed the dynamics of the former MICG mechanism in
416 terms of gravitational multipole formulation, in particular for the sectorial quadrupoles of
417 the MICG system that gives rise to the *Axial Torsional Libration* (ATL) of the inner core
418 (see also Chao and Shih 2021). Based on equating the SYO with ATL, postulating that
419 the shape of the inner core conforms to the equipotential surface under the MICG influ-
420 ence, Shih and Chao (2021) deduced separately the equatorial ellipticity of the inner core
421 and the corresponding sectorial quadrupole of the lower mantle plus CMB. The latter has
422 important implications to the density anomaly associated with the constructs of LLSVP
423 (large low shear velocity provinces; see *e.g.* McNamara (2019), for a review) residing in
424 the lower mantle above the core-mantle boundary. This constitutes a profoundly interest-
425 ing case where space-geodesy observed Earth rotation variations serve as key independent
426 information for the inversion of deep Earth structures found in seismological tomography
427 observations. A more detailed discussion of the LLSVP can be found in Dehant et al., this
428 issue.

429 4 Nutation

430 4.1 Modelling and Observation

431 In practice, the conventional initial precession and nutation model is constructed based on
432 a simplified solid Earth model (Kinoshita 1977). The IAU1980 nutation series (Seidel-
433 mann 1982) are developed from an elastic rotational oceanless Earth model (Wahr 1981).
434 In those products, the contribution from planetary gravitational attraction was originally
435 neglected. It was introduced around the same time by subsequent works (Roosbeek and
436 Dehant 1998; Bretagnon et al. 1998; Hartmann et al. 1999). All those new series for the
437 rigid Earth were truncated at the level of a tenth of a μs and compared with each others.

438 Concerning the non-rigid Earth nutations, with the accumulated VLBI observations
439 (see Sect. 3), the discrepancy between observations and the nutation series IAU1980,
440 which were originally quite significant, has been the object of investigation by several
441 authors (Herring et al. 1991). Zhu et al. (1990) developed a method of covariance analysis

fitting 106 nutation terms, thereby providing corrections to the IAU1980 series. Herring et al. (2002) later estimated the corrections for 21 major nutation terms with respect to the IAU1980 nutation model and the secular trends in longitude and obliquity with respect to the IAU1977 precession rate from a combined series covering the period from 1980 to 2000. These authors then used the resulting VLBI observation series as input to systematically estimate a series of physical effects such as indirect loading, deformations (estimated through compliances) and the core–mantle coupling constants. They used these parameters (named *Basic Earth Parameters*, see below) to build a non-rigid Earth nutation series named MHB2000. This series was adopted by IAU as the IAU2000 nutation model (Soffel et al. 2003). The correction to the precession rate on the IAU2000 values was discussed by Capitaine et al. (2003), which led to updated IAU2006 precession model, using improved polynomial expressions for the precession. These joint initiatives have led to the new IAU2006/2000A precession–nutation model composed of 678 lunisolar and 687 planetary terms induced by the gravitational attraction from the Moon, the Sun, and the other planets.

Updates and corrections to the major IAU2006/2000A nutation component can be found in Gattano et al. (2017) and Zhu et al. (2021). These authors report an average root-mean-square (RMS) errors after correcting some of the nutation harmonic components of about 130 μas and 110 μas , respectively. Both studies are based on IERS 14C04 EOP observations. Figure 10 (based on Zhu et al. 2021) shows the signal residuals which are mostly dominated by the signature of the FCN.

As discussed in the introduction to this work, the FCN is a free rotational mode with a retrograde frequency as measured from the inertial reference frame. Its excitation results from a misalignment between the rotation axis of the Earth's (spheroidal) liquid outer core and the planet's figure axis (see e.g. Requier et al. 2020; Dehant and Mathews 2015). The FCN resonantly amplifies the Earth's response to tidal forcing, as observed in the VLBI data (in the celestial frame) as well as in the retrograde diurnal tidal waves in the records of geophysical sensors in the terrestrial frame (e.g. gravimeters, tiltmeters, strainmeters, etc.); in that latter case, the resonance is designated as the NDFW (see Sect. 2). These resonances have been widely studied by means of VLBI network measurements (Zhu et al. 2021; Herring et al. 1986; Lambert and Dehant 2007; Koot et al. 2008; Rosat and Lambert 2009; Krásná et al. 2013), superconducting gravity records (Florsch and Hinderer 2000; Ducarme et al. 2007; Rosat et al. 2009) or a combination of both (Rosat and Lambert 2009; Ziegler et al. 2020). It is also worth mentioning other experiments performed with strainmeter records (Sato 1991; Zaske et al. 2000; Amoruso et al. 2012; Amoruso and Crescentini 2020) tiltmeters (Riccardi et al. 2018) providing independent, yet somewhat poorer, constraints on the FCN/NDFW parameters. Traces of the FCN are also visible in hydrographic data, demonstrating the observability of the phenomenon long before it was *actually* first observed (Agnew 2018).

The *International VLBI Service (IVS)* is currently working to improve its data through intensive campaigns as well as by developing strategies to balance the current geometry of the VLBI station network. Efforts are also underway in order to incorporate information on the proper motion of distant radio-sources (Lambert 2014). Another source of improvement is provided by the recent reassessment of the influence of atmospheric-oceanic effects on the amplitude of nutations. These have been shown to be particularly important for the prograde annual term (Nurul Huda et al. 2019).

As already mentioned in introduction, in addition to the FCN and FICN resonance effects in the forced nutations, VLBI data feature a contribution from the 'free' FCN mode at the level of a few tenths of mass. The amplitude of this free mode varies with time,

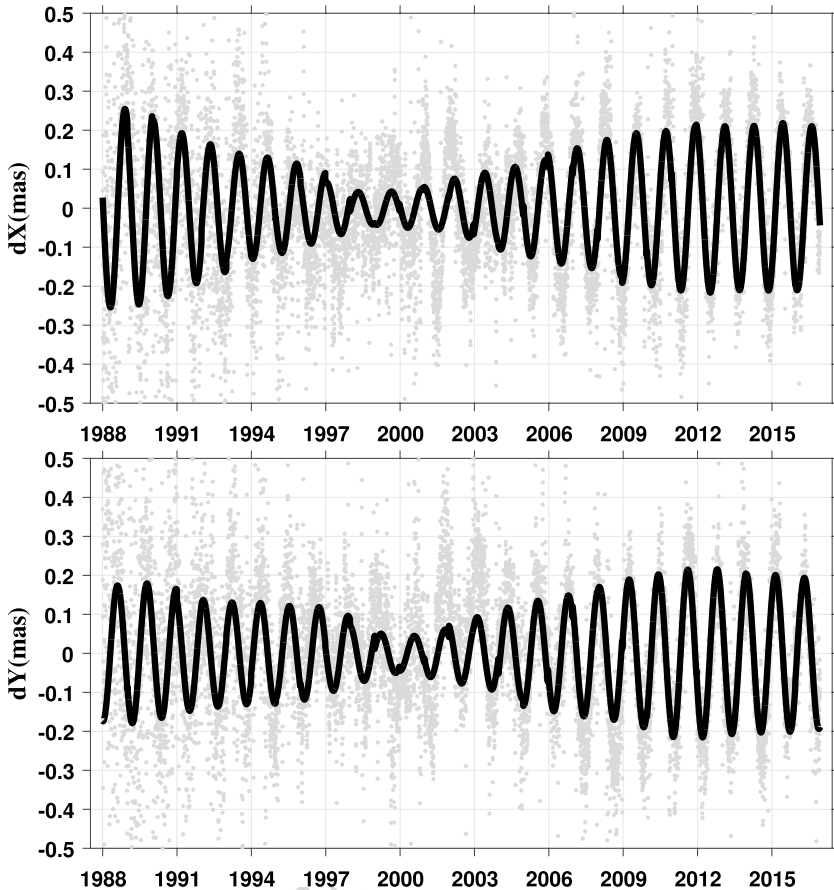


Fig. 10 Nutation residuals from IERS 14C04, which is a combined solution about the IAU2006/IAU2000A precession nutation model. The free core nutation (thick black line) is estimated using an eight years sliding windows

491 which could indicate either a convolution of the free and forced FCN or an interaction
492 between the FCN rotational mode and an inertial mode inside the liquid core (Zhu et al.
493 2021). Although the existence of this kind of interaction is still largely speculative, it has
494 been demonstrated to be theoretically possible by means of numerical simulations (Triana
495 et al. 2019).

496 Similar to the FCN, the FICN could, in principle, be observed via its resonance in diurnal
497 tides and nutations, but the effect being small, it has never been clearly detected yet
498 (Rosat et al. 2016). The only constraints obtained on the FICN are via its influence on the
499 long period 18.6-yr nutation term (Mathews et al. 2002a; Koot et al. 2008; Nurul Huda
500 et al. 2019).

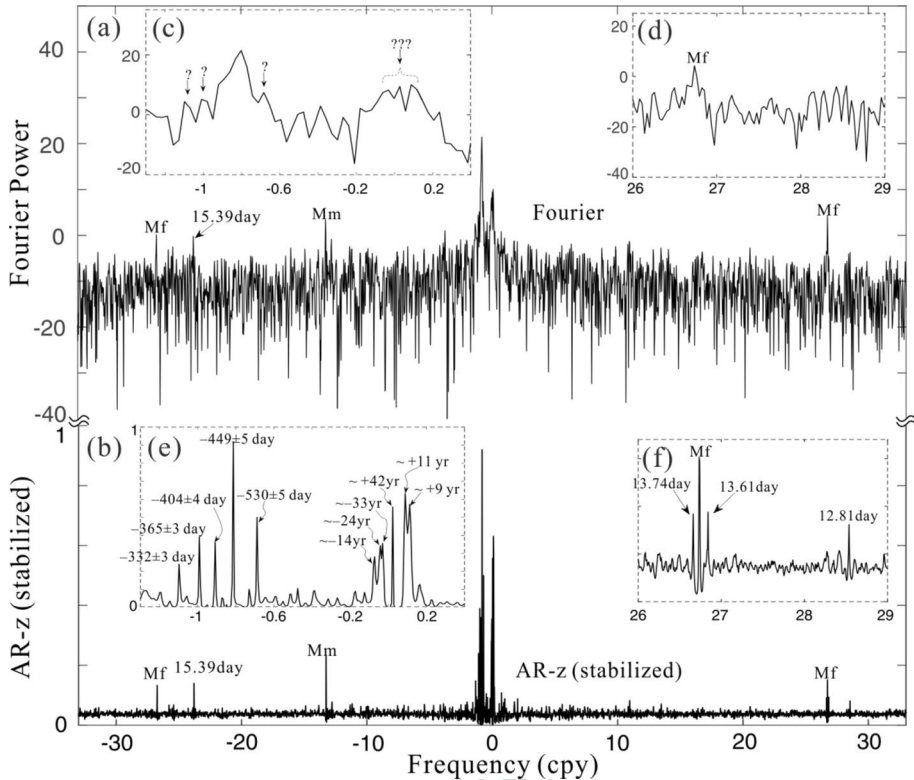


Fig. 11 For the Earth's nutation (1984–2017) in the complex form $\sin \epsilon_0 d\psi(t) + i de(t)$ from VLBI data after all the astronomical nutation terms are removed according to model IAU2000A. (a) Fourier spectrum (logarithmic scale in dB) and (b) stabilized AR-z spectrum. Panels (c), (d), (e), (f) and the inset give the zoom-ins of the frequency bands of interest, (reproduced from [53])

501 **4.2 Interpretations**

502 The nutation series determined from VLBI (see Sect. 4.1) provides the 2-D Earth nutation
 503 motion of the CIP relative to the inertial space in terms of the celestial pole offsets $d\psi$
 504 and de , i.e. the deviations of the longitude ψ and the obliquity ϵ of the equator (relative to
 505 $\epsilon_0 = 23.439^\circ$ the mean obliquity of Earth) in the ecliptic coordinates, or often expressed in
 506 the complex form $\sin \epsilon_0 d\psi(t) + i de(t)$. Or, alternatively, it is simply in terms of the X - and
 507 Y -components of the CIP in space.

508 The free FCN motion is, in principle, the single major signal once all the astronomical
 509 nutation terms are removed according to the state-of-the-art nutation model (see e.g. Zhu
 510 et al. 2021) or the reference model values of IAU2000A (Mathews et al. 2002b). The pre-
 511 sent reference model has a precision of a few mas in the time domain. Only a few nuta-
 512 tion components are not properly determined (see Fig. 10). Fitting the amplitudes of these
 513 ‘new’ components allows us to improve the accuracy of the FCN (and FICN) amplification
 514 parameters in order to obtain new information about the core.

515 Figure 11 shows the power spectrum of $\sin \epsilon_0 d\psi(t) + i de(t)$, where the positive
 516 and negative frequencies correspond to the prograde and retrograde components of the

517 nutational motion in the inertia frame, respectively. Major spectral peaks can be seen in the
 518 Fourier spectrum and can be even more distinctively identified in the stabilized AR-z spec-
 519 trum (Ding and Chao 2018). At longer periods, Fourier and AR-z nutation spectra show
 520 very distinct characteristics (see left portion of the inset of Fig. 11). The Fourier spectrum
 521 shows hardly any identifiable peaks other than that corresponding to the FCN, whereas
 522 the AR-z spectrum exhibits multiple distinctive peaks, among which only two are readily
 523 identifiable: besides the retrograde annual (Sa) nutation as expected, the peak at -449 ± 5
 524 days belongs to the FCN frequency band. It is important to note that the quoted period
 525 here is merely FCN's *apparent* value during the timespan covered by the data. It is close
 526 to but generally not coinciding with the 'true' natural FCN period because it is a result of
 527 convolution of the latter with certain excitation function (Chao and Hsieh 2015). Previ-
 528 ous estimates based on a reconstruction from the tide amplified signal give a value within
 529 the range of -425 to -435 days for the 'true' FCN. A recent estimate by Zhu et al. (2017)
 530 places this value at $T = -429.5 \pm 0.7$ days. Next to the main FCN signal, the presence of
 531 secondary spectral peaks of astronomical nutations at tidal periods indicates the imperfec-
 532 tion of the reference model IAU2000A. Conversely, these findings provide clues for the
 533 reference nutation models.

534 From what precedes, we see that the FCN is the main window to the structure of the
 535 Earth's liquid core as far as nutations are concerned. Comparison between the values of its
 536 frequency and quality factor (*i.e.* its damping) inferred from observation to their theoret-
 537 ical values provides constraints on a number of physical properties. In their simplest form,
 538 these properties are represented by a series of parameters describing the strength of the
 539 coupling between the solid parts of the Earth (mantle and inner core) and its liquid core.
 540 These parameters enter explicitly in the expression of the analytical frequency of the FCN
 541 which reads (Mathews et al. 2002b):

$$542 \quad \frac{\sigma_{\text{FCN}}}{\Omega_0} \simeq - \left(1 + \frac{A_f}{A_m} \right) \left(e_f - \beta + K_{\text{CMB}} + K_{\text{ICB}} \frac{A_s}{A_f} \right), \quad (4)$$

543
 544 where A_m , A_s and A_f denote the principal axis of inertia of the mantle, solid inner core and
 545 fluid outer core, respectively, and e_f is the *dynamical* oblateness of the CMB. Equation (4)
 546 is based on the formalism developed by Sasao et al. (1980) in which the values of the two
 547 (complex) coupling constants, K_{CMB} , and K_{ICB} , parametrize the total torque that comes in
 548 addition to the dynamical pressure torque on the CMB and ICB, respectively (see Dehant
 549 et al. 2017). The imaginary parts of K_{CMB} and K_{ICB} represent the damping of the FCN and
 550 FICN, related to their quality factor Q , and manifesting itself as a phase lag between the
 551 tidal forcing and the induced nutation response. Finally, β is the mantle compliance which
 552 accounts for the elastic response of the mantle. This last parameter is typically estimated
 553 from interior models, as are A_m , A_s , and A_f . Based on this formalism, Gwinn et al. (1986),
 554 and Herring et al. (1986) estimated that the dynamical oblateness of the CMB, e_f , must be
 555 $\sim 5\%$ larger than predicted by hydrostatic interior models. This increase, however, cannot
 556 account on its own for the whole discrepancy between the observed and derived amplitudes
 557 of nutations, nor can it explain the observed phase lag between the tidal forcing and the
 558 nutation response (as e_f is a real number, see above). The complete set of so-called *Basic*
 559 *Earth Parameters* (BEP), e_f , K_{CMB} and K_{ICB} (to which one must add the dynamical flat-
 560 tening of the whole Earth, e), can be estimated from data inversion giving the values pre-
 561 sented in Table 2 updated from Zhu et al. (2017) (see also Koot et al. 2010).

562 Three types of contributions to the value of K_{CMB} are generally considered, namely that
 563 attributed to the fluid core viscosity, the magnetic field and the topography of the CMB

Table 2 Basic Earth parameters determined from VLBI. The period of the FCN is found equal to $T = -429.5 \pm 0.7$ days (see Zhu et al. 2017, for details)

| Parameters | Values | Ranges |
|--|-------------------|------------------|
| $10^3 e$ | 3.2845475 ± 7 | |
| $10^3 (e_f + \text{Re}(K_{\text{CMB}}))$ | 2.6762 ± 7 | [2.67, 2.68] |
| $10^3 \text{Im}(K_{\text{CMB}})$ | -0.0187 ± 4 | [-0.019, -0.018] |
| $10^3 \text{Re}(K_{\text{ICB}})$ | 0.98 ± 3 | [0.95, 1.01] |
| $10^3 \text{Im}(K_{\text{ICB}})$ | -0.92 ± 4 | [-0.96, -0.86] |

(Buffett et al. 2002; Greff-Lefftz and Legros 1995; Koot and Dumberry 2013). The relative contributions of these torques cannot be easily disentangled, primarily because of the large uncertainty that characterizes the shape and electrical conductivity of the lower mantle. Palmer and Smylie (2005) estimated that the viscous torque caused by the molecular viscosity of the liquid core on the CMB is negligible, being 5 orders of magnitude smaller than the estimates for the electromagnetic (EM) torque. The latter is, however, difficult to model due to our poor knowledge of both the electrical conductivity of the lower part of the mantle as well as the intensity of the non-dipolar part of the magnetic field at this location (whereas the non-dipolar part can be inferred from surface measurements, Langel and Estes 1982; Mathews and Guo 2005). Estimates based on the spectral analysis of the harmonics components of large-scale fields place the rms value of the non-dipolar field at about $\sim 0.28\text{mT}$, the same order of magnitude as the dipolar field. Computations of the EM torque based on this value concluded that the EM torque alone could not explain the values of K_{CMB} and K_{ICB} without assuming a magnetic field amplitude not supported by observations even in the very high conductivity limit (Buffett et al. 2002; Mathews and Guo 2005) and regardless of the shape of the non-dipolar field (Koot and Dumberry 2013). This may point towards the need to reassess the contribution from viscosity upwards by invoking the importance of a larger *effective* viscosity at the CMB (Lumb and Aldridge 1991). This possibility was recently suggested again by Triana et al. (2021) based on their computational estimate of the FCN decay rate due to ohmic and viscous dissipation.

Another ingredient that could potentially complement the effects of the viscous and EM torques is the *topographic torque* produced by the pressure forces within the fluid on a 'rough' CMB. Formally, any deviation of the CMB from an elliptical surface should alter the shape of the flow inside the core, causing it to deviate from the simple solid-body rotation traditionally assumed when modelling the FCN (see Sect. 5). When the amplitude of the CMB topography is small, its effect can be treated as a perturbation. This is the view taken by Wu and Wahr (1997) who predicted a deviation of about 0.2mas on the amplitude of the retrograde annual nutation caused by the small shift in the FCN frequency. However, their results depend strongly on the model of CMB topography chosen. More work is needed to link together the results obtained on the topography with those mentioned above (see also Dehant et al. 2012, on the subject).

Finally, there is the possibility that the FCN might be influenced by the presence of other free modes with nearby frequencies, the natural candidates being *Inertial Modes* of which the FCN is the simplest representative (Rekier et al. 2020; Triana et al. 2021; Rekier et al. 2019). Triana et al. (2019) have shown how these modes can interact in a non-trivial way when the viscosity and ratio of moments of inertia of the core and mantle are such that the FCN frequency and damping are close to that of some other mode thereby causing a shift in the values of the former. Although the regime of parameters at which such

602 interactions can take place is far from that relevant to the Earth, it might theoretically be
603 reachable when the magnetic field is taken into account (Triana et al. 2019).

604 5 Conclusion and Prospects

605 Earth's rotation signal covers a broad range of time-scales and contains fundamental infor-
606 mation related to deep Earth's processes. The study of these processes is complicated
607 by the influence of surficial processes related to geophysical fluids (*i.e.* the oceans and
608 atmosphere) that also affect PM, LOD and nutations thus masking smaller core signals.
609 Combined geodetic, magnetic and gravimetric observations have already provided signifi-
610 cant constraints on the physics of the outer core boundary. On the other hand, our current
611 knowledge of the inner core is still limited.

612 Regarding PM and Δ LOD, satellite gravity measurements from GRACE and GRACE
613 Follow-On (GFO) offer a revolutionary means of measuring large-scale mass changes in
614 the climate system, especially those associated with the global hydrological cycle (Tapley
615 et al. 2019), and can help improve the quantification and interpretation of geophysical exci-
616 tations of Δ LOD and PM (Chen et al. 2016; Götzl et al. 2018; Nastula et al. 2019). GRACE/
617 GFO have collected nearly two decades of time-variable satellite gravity measurements so
618 far, and the series are expected to be extended to well over 20 years (possibly 30). With the
619 future generations of GRACE missions that are under planning, satellite gravimetry will
620 bring a new era of studying geophysical excitations of Δ LOD and PM with unprecedented
621 accuracy. The existence of a 5.9-year variation (SYO) in both PM and Δ LOD signals is
622 intriguing. Although the SYO is almost completely accounted for by surface processes
623 for PM, this is not the case for Δ LOD for which the removal of the AOH contribution
624 only makes the SYO appear more clearly. This hints towards a possible deep interior ori-
625 gin, likely interactions between the core and mantle. In this respect, development of more
626 accurate surficial models (especially in hydrology) and continuous, ever more precise,
627 space observations cannot miss to provide new insights on core processes in the future. As
628 regards the theoretical understanding that this will provide, progress in the near future will
629 most likely come from a better characterization of the interannual oscillations in LOD and
630 PM driven by interactions between the core and mantle. A unified model of these oscilla-
631 tions and how they might relate to core processes that also affect long period nutations (*e.g.*
632 geomagnetic jerks) is still lacking at the moment and would prove very valuable.

633 Regarding nutations, continued VLBI observations of nutations will secure the determi-
634 nation of the forced nutation amplitudes in general and the 18.6-year nutation in particular.
635 These nutations are essential to derive the values of the BEP (see Table 2). To be more
636 exact, the BEP allows to determine the imaginary part of the coupling constants, K_{CMB}
637 and K_{ICB} , as well as a combination of the core dynamical flattening, e_f , and the real part of
638 the coupling constant (see Eq. 4). As we already discussed in Sect. 4.2, the relative impor-
639 tance of these parameters cannot be disentangled without making additional hypotheses as
640 regard the nature and dynamics of the flow inside the Earth's core. Therefore, improvement
641 in the current nutation model will necessarily come from a combination of improved meas-
642 urements and theoretical exploration. The present model currently relies on the following
643 assumptions:

- 644 (a) The angular momentum of the liquid core is equal to that of an inviscid non-magnetic
645 and neutrally buoyant flow with uniform vorticity (*a.k.a.* Poincaré flow)

- 646 (b) The outer core exchanges angular momentum with the inner core and the mantle via
647 the (dynamic) pressure and electromagnetic torques acting on the ICB and the CMB,
648 both of which approximated as oblate spheroidal surfaces
- 649 (c) The damping of the FCN is attributed to the ohmic dissipation inside a thin electrically
650 conducting layer at the base of the mantle

651 As we already discussed in Sect. 4.2, (a) is well supported by the theoretical study of inertial
652 modes which may be seen as the basis of the fluid motion inside the core (Ivers 2017).
653 However, this simple picture is currently challenged by recent studies that show how angu-
654 lar momentum can be transported through the core when the effects of viscosity, magnetic
655 field and density stratification are taken into account, thereby also questioning both (b) and
656 (c) (see Triana et al., this issue). In the nearest future, progress will most likely come from
657 a detailed reassessment of the viscous and electromagnetic couplings at the CMB. Efforts
658 in this direction are currently undertaken within the GRACEFUL project.

659 **Acknowledgements** We would like to extend our gratitude to the anonymous reviewers whose comments
660 helped to significantly improve the quality of our manuscript. The International Space Science Institute
661 (ISSI) is gratefully acknowledged for the support in organizing the workshop that has led to the writing
662 of this paper. The research leading to the results provided by VD, JR and PZ for this paper has received
663 funding from the European Research Council (ERC) under the European Union's Horizon 2020 research
664 and innovation programme (RotaNut Advanced Grant 670874 + GRACEFUL Synergy Grant agreement No
665 855677).

666 **Declarations**

667 **Conflict of interest** The authors declare that they have no conflict of interest.

668 **References**

- 669 Abarca del Rio R, Gambis D, Salstein D (2000) Interannual signals in length of day and atmospheric angu-
670 lar momentum. *Ann Geophys* 18:347–364
- 671 Adhikari S, Ivins ER (2016) Climate-driven polar motion: 2003–2015. *Sci Adv* 2(4)
- 672 Agnew DC (2018) An improbable observation of the diurnal core resonance. *Pure Appl Geophys*
673 175(5):1599–1609
- 674 Amoruso A, Crescentini L (2020) Parameters of the earth's free core nutation from diurnal strain tides. *Sci*
675 *Rep* 10(1)
- 676 Amoruso A, Botta V, Crescentini L (2012) Free core resonance parameters from strain data: sensitivity
677 analysis and results from the gran sasso (italy) extensometers. *Geophys Jo Int* 189(2):923–936
- 678 Aubert J, Finlay CC (2019) Geomagnetic jerks and rapid hydromagnetic waves focusing at Earth's core sur-
679 face. *Nat Geosci* 12(5):393–398
- 680 Ball R, Kahle A, Vestine E (1969) Determination of surface motions of the Earth's core. *J Geophys Res*
681 74(14)
- 682 Barnes RTH, Hide R, White AA, Wilson CA (1983) Atmospheric angular momentum fluctuations, length-
683 of-day changes and polar motion. *Proc Royal Soc London Series A Math Phys Sci* 387(1792):31–73
- 684 Benjamin D, Wahr J, Ray R, Egbert G, Desai S (2006) Constraints on mantle anelasticity from geodetic
685 observations, and implications for the J2 anomaly. *Geophys J Int* 165(1):3–16
- 686 Bizouard C (2020) *Geophysical Modelling of the Polar Motion*. De Gruyter, Berlin, Boston
- 687 Bizouard C, Nurul Huda I, Ziegler Y, Lambert S (2019) Frequency dependence of the polar motion reso-
688 nance. *Geophys J Int* 220(2):753–758
- 689 Bloxham J, Jackson A (1991) Fluid flow near the surface of earth's outer core. *Rev Geophys* 29(1):97–120
- 690 Bretagnon P, Franou G, Rocher P, Simon J (1998) Smart97: a new solution for the rotation of the rigid
691 earth. *Astron Astrophys* 329:329–338
- 692 Buffett B, Mathews P, Herring T (2002) Modeling of nutation and precession: effects of electromagnetic
693 coupling. *J Geophys Res* 107(B4):5.1–5.14:5.1–5.14

- 694 Buffett BA (1996) A mechanism for decade fluctuations in the length of day. *Geophys Res Lett*
695 23(25):3803–3806
- 696 Buffett BA, Mound J, Jackson A (2009) Inversion of torsional oscillations for the structure and dynamics of
697 Earth's core. *Geophys J Int* 177(3):878–890
- 698 Capitaine N, Wallace PT, Chapront J (2003) Expressions for iau 2000 precession quantities. *Astron Astro-*
699 *phys* 412(2):567–586
- 700 Chao B, Hsieh Y (2015) The earth's free core nutation: formulation of dynamics and estimation of eigenpe-
701 riod from the very-long-baseline interferometry data. *Earth Planet Sci Lett* 432:483–492
- 702 Chao B, Yu Y (2020) Variation of the equatorial moments of inertia associated with a 6-year westward
703 rotary motion in the Earth. *Earth Planet Sci Lett* 542:116316
- 704 Chao BF (1985) On the excitation of the Earth' polar motion. *Geophys Res Lett* 12(8):526–529
- 705 Chao BF (1989) Length-of-day variations caused by el niño-southern oscillation and quasi-biennial oscilla-
706 tion. *Science* 243(4893):923–925. <https://doi.org/10.1126/science.243.4893.923>
- 707 Chao BF (2017) Dynamics of axial torsional libration under the mantle-inner core gravitational interaction.
708 *J Geophys Res Solid Earth* 122:560–571
- 709 Chao BF, Gross RS (1987) Changes in the earth's rotation and low-degree gravitational field induced by
710 earthquakes. *Geophys J Int* 91(3):569–596
- 711 Chao BF, Shih SA (2021) Multipole expansion: unifying formalism for earth and planetary gravitational
712 dynamics. *Surv Geophys*. <https://doi.org/10.1007/s10712-021-09650-8>
- 713 Chao BF, Chung W, Shih Z, Hsieh Y (2014) Earth's rotation variations: a wavelet analysis. *Terra Nova*
714 26:260–264
- 715 Chen J, Wilson CR, Kuang W, Chao BF (2019) Interannual oscillations in Earth Rotation. *J Geophys Res*
716 *Solid Earth* 124(12):13404–13414
- 717 Chen JL, Wilson CR (2005) Hydrological excitations of polar motion, 1993–2002. *Geophys J Int*
718 160(3):833–839
- 719 Chen JL, Wilson CR, Chao BF, Shum CK, Tapley BD (2000) Hydrological and oceanic excitations to polar
720 motion and length-of-day variation. *Geophys J Int* 141(1):149–156
- 721 Chen JL, Wilson CR, Ries JC, Tapley BD (2013) Rapid ice melting drives earth's pole to the east. *Geophys*
722 *Res Lett* 40(11):2625–2630
- 723 Chen JL, Wilson CR, Ries JC (2016) Broadband assessment of degree-2 gravitational changes from grace
724 and other estimates, 2002–2015. *J Geophys Res Solid Earth* 121(3):2112–2128
- 725 Davies CJ, Stegman DR, Dumberry M (2014) The strength of gravitational core-mantle coupling. *Geophys*
726 *Res Lett* 41(11):3786–3792. <https://doi.org/10.1002/2014GL059836>
- 727 de Viron O, Bizouard C, Salstein D, Dehant V (1999) Atmospheric torque on the earth rotation and compar-
728 ison with atmospheric angular momentum variations. *J Geophys Res* 104(B3):4861–4875
- 729 de Viron O, Ponte R, Dehant V (2001) Atmospheric torque on the earth rotation and comparison with
730 atmospheric angular momentum variations. *J Geophys Res* 106(B5):8841–8851
- 731 Defraigne P, Smits I (1999) Length of day variations due to zonal tides for an inelastic earth in non-hydro-
732 static equilibrium. *Geophys J Int* 139(2):563–572
- 733 Dehant V, Mathews P (2015) *Precession, Nutation, and Wobble of the Earth*. Cambridge University Press,
734 Cambridge, p 536
- 735 Dehant V, Folgueira M, Puica M (2012) Analytical computation of the effects of the core-mantle boundary
736 topography on tidal length-of-day variations. *Proc Journées Systèmes de Référence spatio-temporels*
737 2011, Vienna, Austria pp 113–116
- 738 Dehant V, Laguerre R, Requier J, Rivoldini A, Triana SA, Trinh A, Van Hoolst T, Zhu P (2017) Understand-
739 ing the effects of the core on the nutation of the Earth. *Geodesy Geodyn* 8(6):389–395
- 740 Ding H, Chao BF (2018) A 6-year westward rotary motion in the earth: detection and possible MICG cou-
741 pling mechanism. *Earth Planet Sci Lett* 495:50–55
- 742 Ding H, Pan Y, Xu XY, Shen W, Li M (2019) Application of the AR-z spectrum to polar motion: a possible
743 first detection of the inner core wobble and its implications for the density of earth's core. *Geophys*
744 *Res Lett* 46(23):13765–13774
- 745 Ding H, An Y, Shen W (2021) New evidence for the fluctuation characteristics of intradecadal periodic
746 signals in length-of-day variation. *J Geophys Res Solid Earth*. <https://doi.org/10.1029/2020JB020990>
- 747 Dobslaw H, Dill R (2018) Predicting earth orientation changes from global forecasts of atmosphere-hydro-
748 sphere dynamics. *Adv Space Res* 61(4):1047–1054
- 749 Duan P, Huang C (2020) Intradecadal variations in length of day and their correspondence with geomag-
750 netic jerks. *Nat Commun* 11:2273. <https://doi.org/10.1038/s41467-020-16109-8>
- 751 Duan P, Liu G, Liu L, Hu X, Hao X, Huang Y, Zhang Z, Wang B (2015) Recovery of the 6-year signal
752 in length of day and its long-term decreasing trend. *Earth Planet Space*. <https://doi.org/10.1186/s40623-015-0328-6>
- 753

- 754 Ducarme B, Sun HP, Xu J (2007) Determination of the free core nutation period from tidal gravity observa-
755 tions of the GGP superconducting gravimeter network. *J Geodyn* 81:179–187
- 756 Dumberry M, Bloxham J (2006) Azimuthal flows in the earth's core and changes in length of day at millen-
757 nial timescales. *Geophys J Int* 165(1):32–46
- 758 Fey AL, Gordon D, Jacobs CS, Ma C, Gaume RA, Arias EF, Bianco G, Boboltz DA, Böckmann S, Bolotin
759 S, Charlot P, Collioud A, Engelhardt G, Gipson J, Gontier AM, Heinkelmann R, Kurubov S, Lam-
760 bert S, Lytvyn S, MacMillan DS, Malkin Z, Nothnagel A, Ojha R, Skurikhina E, Sokolova J, Souchay
761 J, Sovers OJ, Tesmer V, Titov O, Wang G, Zharov V (2015) The second realization of the interna-
762 tional celestial reference frame by very long baseline interferometry. *The Astron J* 150(2):58. <https://doi.org/10.1088/0004-6256/150/2/58>
- 763 Florsch N, Hinderer J (2000) Bayesian estimation of the free core nutation parameters from the analysis of
764 precise tidal gravity data. *Phys Earth Planet Inter* 117(1):21–35
- 765 Gattano C, Lambert SB, Bizouard C (2017) Observation of the earth's nutation by the vlbi: how accurate is
766 the geophysical signal. *J Geodesy* 91(7):849–856
- 767 Gillet N, Jault D, Canet E, Fournier A (2010) Fast torsional waves and strong magnetic field within the
768 Earth's core. *Nature* 465(7294):74–77
- 769 Göttl F, Schmidt M, Seitz F (2018) Mass-related excitation of polar motion: an assessment of the new RL06
770 GRACE gravity field models. *Earth Planet Space* 70(1):195
- 771 Greff-Lefftz M, Legros H (1995) Core-mantle coupling and polar motion. *Phys Earth Planet Inter*
772 91(4):273–283
- 773 Gross R (2015) 3.09 - earth rotation variations - long period. In: Schubert G (ed) *Treatise on Geophysics*
774 (Second Edition), second, edition. Elsevier, Oxford, pp 215–261
- 775 Gross RS, Chao BF (2006) The rotational and gravitational signature of the December 26, 2004 Sumatran
776 earthquake. *Surv Geophys* 27(6):615–632
- 777 Gross RS, Fukumori I, Menemenlis D, Gegout P (2004) Atmospheric and oceanic excitation of length-of-
778 day variations during 1980–2000. *J Geophys Res Solid Earth* 109(B1)
- 779 Guo JY, Greiner-Mai H, Ballani L (2005) A spectral search for the inner core wobble in Earth's polar
780 motion. *J Geophys Res Solid Earth* 110(B10)
- 781 Gwinn CR, Herring TA, Shapiro II (1986) Geodesy by radio interferometry: studies of the forced nuta-
782 tions of the Earth: 2. Interpretation. *J Geophys Res* 91(B5):4755. [https://doi.org/10.1029/JB091iB05p](https://doi.org/10.1029/JB091iB05p04755)
783 [04755](https://doi.org/10.1029/JB091iB05p04755)
- 784 Hartmann T, Soffel M, Ron C (1999) The geophysical approach towards the nutation of a rigid earth. *Astron*
785 *Astrophys Suppl Ser* 134(2):271–286
- 786 Herring T, Mathews P, Buffett B (2002) Modeling of nutation-precession: Very long baseline interferometry
787 results. *J Geophys Res Solid Earth* 107(B4):ETG–4
- 788 Herring TA, Gwinn CR, Shapiro II (1986) Geodesy by radio interferometry: studies of the forced nutations
789 of the Earth: 1. Data analysis. *J Geophys Res* 91(B5):4745–4754
- 790 Herring TA, Buffett BA, Mathews P, Shapiro II (1991) Forced nutations of the earth: influence of inner core
791 dynamics: 3. very long interferometry data analysis. *J Geophys Res Solid Earth* 96(B5):8259–8273
- 792 Hide R (1969) Interaction between the earth's liquid core and solid mantle. *Nature* 222:599–607
- 793 Hide R, Clayton RW, Hager BH, Spieth MA, Voorhdes CV (1993) Topographic Core-Mantle Coupling and
794 Fluctuations in the Earth's Rotation, American Geophysical Union (AGU), pp 107–120
- 795 Hide R, Boggs DH, Dickey JO, Dong D, Gross RS, Jackson A (1996) Topographic core-mantle coupling
796 and polar motion on decadal time-scales. *Geophys J Int* 125(2):599–607
- 797 Holme R (1998) Electromagnetic core-mantle coupling-i. explaining decadal changes in the length of day.
798 *Geophys J Int* 132(1):167–180
- 799 Holme R, De Viron O (2013) Characterization and implications of intradecadal variations in length of day.
800 *Nature* 499:202–204
- 801 Hsu CC, Duan PS, Xu XQ, Zhou YH, Huang CL (2021) On the ~7 year periodic signal in length of day
802 from a frequency domain stepwise regression method. *J Geodesy* 95:55. [https://doi.org/10.1007/](https://doi.org/10.1007/s00190-021-01503-x)
803 [s00190-021-01503-x](https://doi.org/10.1007/s00190-021-01503-x)
- 804 Ivers D (2017) Enumeration, orthogonality and completeness of the incompressible Coriolis modes in a
805 tri-axial ellipsoid. *Geophys Astrophys Fluid Dyn* 111(5):333–354. [https://doi.org/10.1080/03091929.](https://doi.org/10.1080/03091929.2017.1330412)
806 [2017.1330412](https://doi.org/10.1080/03091929.2017.1330412)
- 807 Ivins ER, James TS (2005) Antarctic glacial isostatic adjustment: a new assessment. *Antarctic Sci* 17(4):541
- 808 Jault D, Le Mouél JL (1990) Core-mantle boundary shape: constraints inferred from the pressure torque act-
809 ing between the core and the mantle. *Geophys J Int* 101(1):233–241
- 810 Jault D, Gire C, Le Mouél JL (1988) Westward drift, core motions and exchanges of angular momentum
811 between core and mantle. *Nature* 333(6171):353–356
- 812 Kinoshita H (1977) Theory of the rotation of the rigid earth. *Celes Mech* 15(3):277–326
- 813

- 814 Koot L, Dumberry M (2013) The role of the magnetic field morphology on the electromagnetic coupling for
815 nutations. *Geophys J Int* 195(1):200–210
- 816 Koot L, Rivoldini A, de Viron O, Dehant V (2008) Estimation of earth interior parameters from a Bayesian
817 inversion of very long baseline interferometry nutation time series. *J Geophys Res* 113(B08414)
- 818 Koot L, Dumberry M, Rivoldini A, de Viron O, Dehant V (2010) Constraints on the coupling at the core-
819 mantle and inner core boundaries inferred from nutation observations. *Geophys J Int* 182:1279–1294
- 820 Krásná H, Böhm J, Schuh H (2013) Free core nutation observed by VLBI. *Astron Astrophys* 555:29
- 821 Kuang W, Chao BF, Chen J (2019) Reassessment of electromagnetic core-mantle coupling and its implica-
822 tions to the Earth's decadal polar motion. *Geodesy Geodyn* 10(5):356–362
- 823 Lambert SB (2014) Comparison of VLBI radio source catalogs. *Astron Astrophys* 570:108
- 824 Lambert SB, Dehant V (2007) The Earth's core parameters as seen by the VLBI. *Astron Astrophys*
825 469:777–781
- 826 Langel RA, Estes RH (1982) A geomagnetic field spectrum. *Geophys Res Lett* 9(4):250–253. <https://doi.org/10.1029/GL009i004p00250>
- 827
- 828 Lumb LI, Aldridge KD (1991) On viscosity estimates for the Earth's fluid outer core and core-mantle cou-
829 pling. *J Geomag Geoelectr* 43(2):93–110. <https://doi.org/10.5636/jgg.43.93>
- 830 Malkin ZM (2020) Statistical analysis of the results of 20 years of activity of the international VLBI service
831 for geodesy and astrometry. *Astron Rep* 64(2):168–188
- 832 Manda M, Holme R, Pais A, Pinheiro K, Jackson A, Verbanac G (2010) Geomagnetic jerks: rapid core
833 field variations and core dynamics. *Space Sci Rev* 155(1–4):147–175
- 834 Markowitz W (1960) Latitude and longitude, and the secular motion of the pole. *Methods Tech Geophys pp*
835 325–361
- 836 Markowitz W (1961) International determination of the total motion of the pole. *Bul Geod* 59:29–41
- 837 Mathews P, Herring TA, Buffett BA (2002a) Modeling of nutation precession: new nutation series for non-
838 rigid Earth and insights into the Earth's interior. *J Geophys Res* 107(B4):ETG3–1–3–30
- 839 Mathews PM, Bretagnon P (2003) Polar motions equivalent to high frequency nutations for a nonrigid
840 Earth with anelastic mantle. *Astron Astrophys* 400(3):1113–1128. <https://doi.org/10.1051/0004-6361:20021795>
- 841
- 842 Mathews PM, Guo JY (2005) Viscoelectromagnetic coupling in precession-nutation theory. *J Geophys Res*
843 *Solid Earth*. 10.1029/2003JB002915
- 844 Mathews PM, Herring TA, Buffett BA (2002b) Modeling of nutation and precession: new nuta-
845 tion series for nonrigid earth and insights into the earth's interior. *J Geophys Res Solid Earth*.
846 10.1029/2001JB000390
- 847 McNamara AK (2019) A review of large low shear velocity provinces and ultra low velocity zones. *Tec-
848 tonophysics* 760:199–220
- 849 Mitrovica JX, Hay CC, Morrow E, Kopp RE, Dumberry M, Stanley S (2015) Reconciling past changes
850 in Earth's rotation with 20th century global sea-level rise: resolving Munk's enigma. *Sci Adv*
851 1(11):e1500679. <https://doi.org/10.1126/sciadv.1500679>
- 852 Mound J, Buffett B (2003) Interannual oscillations in length of day: Implications for the structure of the
853 mantle and core. *J Geophys Res Solid Earth* 108(B7)
- 854 Mound JE, Buffett BA (2006) Detection of a gravitational oscillation in length-of-day. *Earth Planet Sci Lett*
855 243(3):383–389
- 856 Munk W (1997) Once again: once again-tidal friction. *Prog Oceanogr* 40(1–4):7–35
- 857 Munk W, MacDonald G (1960) *The Rotation of the Earth: a Geophysical Discussion*. Cambridge Univ
858 Press, Cambridge
- 859 Nastula J, Ponte RM, Salstein DA (2007) Comparison of polar motion excitation series derived from grace
860 and from analyses of geophysical fluids. *Geophys Res Lett* 34(11)
- 861 Nastula J, Wińska M, Śliwińska J, Salstein D (2019) Hydrological signals in polar motion excitation - evi-
862 dence after fifteen years of the grace mission. *J Geodyn* 124:119–132
- 863 Nurul Huda I, Lambert S, Bizouard C, Ziegler Y (2019) Nutation terms adjustment to vlbi and implication
864 for the earth rotation resonance parameters. *Geophys J Int* 220(2):759–767
- 865 Palmer A, Smylie D (2005) Vlbi observations of free core nutations and viscosity at the top of the core.
866 *Phys Earth Planet Inter* 148(2):285–301. <https://doi.org/10.1016/j.pepi.2004.09.003>
- 867 Peltier W (2004) Global glacial isostasy and the surface of the ice-age earth: the ice-5g (vm2) model and
868 grace. *Ann Rev Earth Planet Sci* 32(1):111–149
- 869 Peltier W (2007) History of earth rotation. *Treatise Geophys* 9:243–293
- 870 Peltier W, Jiang X (1996) Glacial isostatic adjustment and earth rotation: refined constraints on the viscosity
871 of the deepest mantle. *J Geophys Res Solid Earth* 101(B2):3269–3290
- 872 Ray RD, Erofeeva SY (2014) Long-period tidal variations in the length of day. *J Geophys Res Solid Earth*
873 119(2):1498–1509

- 874 Requier J, Trinh A, Triana SA, Dehant V (2019) Inertial modes in near-spherical geometries. *Geophys J Int*
875 216(2):777–793. <https://doi.org/10.1093/gji/ggy465>
- 876 Requier J, Triana SA, Trinh A, Dehant V (2020) Inertial modes of a freely rotating ellipsoidal planet and their
877 relation to nutations. *Planet Sci J* 1(1):20
- 878 Riccardi U, Boy JP, Hinderer J, Rosat S, Boudin F (2018) Free Core Nutation Parameters from Hydrostatic
879 Long-Base Tiltmeter Records in Sainte Croix aux Mines (France). In: Freymueller, JT and Sanchez, L
880 (ed) International Symposium on Earth and Environmental Sciences for Future Generations, International
881 Association of Geodesy Symposia, vol 147, pp 171–179
- 882 Roosbeek F, Dehant V (1998) Rdan97: an analytical development of rigid earth nutation series using the
883 torque approach. *Celest Mech Dyn Astron* 70(4):215–253
- 884 Rosat S, Hinderer J (2018) Limits of Detection of Gravimetric Signals on Earth. *Sci Rep* 8(1):15324. <https://doi.org/10.1038/s41598-018-33717-z>
- 885 Rosat S, Lambert SB (2009) Free core nutation resonance parameters from VLBI and superconducting
886 gravimeter data. *Astron Astrophys* 503:287–291
- 887 Rosat S, Florsch N, Hinderer J, Llubes M (2009) Estimation of the free core nutation parameters from SG
888 data: sensitivity study and comparative analysis using linearized Least-Squares and Bayesian meth-
889 ods. *J Geodyn* 48:331–339
- 890 Rosat S, Calvo M, Lambert S (2016) Detailed Analysis of Diurnal Tides and Associated Space Nutation in
891 the Search of the Free Inner Core Nutation Resonance. In: Freymueller J, Sánchez L (eds) International
892 Symposium on Earth and Environmental Sciences for Future Generations, Springer, International
893 Association of Geodesy Symposia, vol 147
- 894 Rosat S, Gillet N, Boy JP, Couhert A, Dumberry M (2020) Interannual variations of degree 2 from geodetic
895 observations and surface processes. *Geophys J Int.* 10.1093/gji/ggaa590
- 896 Rosen RD, Salstein DA (1983) Variations in atmospheric angular momentum on global and regional scales
897 and the length of day. *J Geophys Res Oceans* 88(C9):5451–5470
- 898 Sasao T, Okubo S, Saito M (1980) A Simple Theory on the Dynamical Effects of a Stratified Fluid Core
899 upon Nutational Motion of the Earth. Springer, Netherlands, Dordrecht, pp 165–183
- 900 Sato T (1991) Fluid core resonance measured by quartz tube extensometers at Esashi earth tide station. In:
901 Kakkuri J (ed) Proceedings of the 11th International Symposium on Earth tides, pp 573–582
- 902 Schuh H, Behrend D (2012) Vlbi: a fascinating technique for geodesy and astrometry. *J Geodyn* 61:68–80
- 903 Seidelmann P (1982) 1980 iau theory of nutation: the final report of the iau working group on nutation.
904 *Celest Mech* 27(1):79–106
- 905 Shih SA, Chao BF (2021) Inner core and its libration under gravitational equilibrium: implications to lower-
906 mantle density anomaly. *J Geophys Res Solid Earth*. 10.1029/2020JB020541
- 907 Silva L, Jackson L, Mound J (2012) Assessing the importance and expression of the 6 year geomagnetic
908 oscillation. *J Geophys Res Solid Earth* 117(B10)
- 909 Soffel M, Klioner SA, Petit G, Wolf P, Kopeikin S, Bretagnon P, Brumberg V, Capitaine N, Damour T,
910 Fukushima T et al (2003) The iau 2000 resolutions for astrometry, celestial mechanics, and metrology
911 in the relativistic framework: explanatory supplement. *The Astron J* 126(6):2687
- 912 Stephenson F, Morrison L, Hohenkerk C (2016) Measurement of the earth's rotation: 720 bc to ad
913 2015. In: Proceedings of the Royal Society A: Mathematical, Physical and Engineering Sciences
914 472(2196):20160404
- 915 ...Tapley BD, Watkins MM, Flechtner F, Reigber C, Bettadpur S, Rodell M, Sasgen I, Famiglietti JS, Lan-
916 derer FW, Chambers DP, Reager JT, Gardner AS, Save H, Ivins ER, Swenson SC, Boening C, Dahle
917 C, Wiese DN, Dobslaw H, Tamisiea ME, Velicogna I (2019) Contributions of GRACE to understand-
918 ing climate change. *Nat Clim Change* 9(5):358–369
- 919 Triana S, Requier J, Trinh A, Dehant V (2019) The coupling between inertial and rotational eigenmodes in
920 planets with liquid cores. *Geophys J Int* 218:375–389
- 921 Triana SA, Trinh A, Requier J, Zhu P, Dehant V (2021) The viscous and ohmic damping of the earth's free
922 core nutation. *J Geophys Res Solid Earth* 126(4):1–14
- 923 Wahr JM (1981) The forced nutations of an elliptical, rotating, elastic and oceanless earth. *Geophys J Int*
924 64(3):705–727
- 925 Van der Wal W, Schotman H, Vermeersen L (2004) Geoid heights due to a crustal low viscosity zone in gla-
926 cial isostatic adjustment modeling: a sensitivity analysis for goce. *Geophys Res Lett* 31(5)
- 927 Wu P, Peltier W (1984) Pleistocene deglaciation and the earth's rotation: a new analysis. *Geophys J Int*
928 76(3):753–791
- 929 Wu X, Wahr J (1997) Effects of non-hydrostatic core-mantle boundary topography and core dynamics on
930 earth rotation. *Geophys J Int* 128:18–42
- 931 Xu CY, Chao BF (2019) Seismic effects on the secular drift of the earth's rotational pole. *J Geophys Res*
932 *Solid Earth* 124(6):6092–6100. <https://doi.org/10.1029/2018JB017164>
- 933

Surveys in Geophysics

- 934 Zaske J, Zürn W, Wilhelm H (2000) NDFW analysis of Borehole water level data from the hot-dry-rock test
935 site soultz-sous-forêts. *Bull d'Information des Marées Terrestres* 132:10241–10270
- 936 Zhu P, Rivoldini A, Koot L, Dehant V (2017) Basic earth's parameters as estimated from vlbi observations.
937 *Geodesy Geodyn* 8(6):427–432
- 938 Zhu P, Triana SA, Requier J, Trinh A, Dehant V (2021) Quantification of corrections for the main lunisolar
939 nutation components and analysis of the free core nutation from vlbi observed nutation residuals. *J*
940 *Geodesy*. <https://doi.org/10.1007/s00190-021-01513-9>
- 941 Zhu S, Groten E, Reigber C (1990) Various aspects of numerical determination of nutation constants. ii-an
942 improved nutation series for the deformable earth. *The Astron J* 99:1024–1044
- 943 Ziegler Y, Hinderer J, Rogister Y, Rosat S (2016a) Estimation of the gravimetric pole tide by stacking long
944 time-series of GGP superconducting gravimeters. *Geophys J Int* 205(1):77–88
- 945 Ziegler Y, Rogister Y, Hinderer J, Rosat S (2016b) Chandler Wobble and Frequency Dependency of the
946 Ratio Between Gravity Variation and Vertical Displacement for a Simple Earth Model with Maxwell
947 or Burgers Rheologies. In: JT F, L S (eds) *International Symposium on Earth and Environmental*
948 *Sciences for Future Generations*, Springer, International Association of Geodesy Symposia, vol 147
- 949 Ziegler Y, Lambert SB, Huda IN, Bizouard C, Rosat S (2020) Contribution of a joint Bayesian inversion
950 of VLBI and gravimetric data to the estimation of the free inner core nutation and free core nutation
951 resonance parameters. *Geophys J Int* 222(2):845–860

952 **Publisher's Note** Springer Nature remains neutral with regard to jurisdictional claims in published maps and
953 institutional affiliations.

954

UNCORRECTED PROOF